AMERICAN SOCIETY FOR MICROBIOLOGY | Infection and Immunity®

CELLULAR MICROBIOLOGY:
PATHOGEN-HOST CELL MOLECULAR INTERACTIONS

The Host GTPase Arf1 and Its Effectors AP1 and PICK1 Stimulate Actin Polymerization and Exocytosis To Promote Entry of *Listeria monocytogenes*

Susan Saila,[a] Gaurav Chandra Gyanwali,[a] Mazhar Hussain,[a] Antonella Gianfelice,[a] Keith Ireton[a]

[a]Department of Microbiology and Immunology, University of Otago, Dunedin, New Zealand

ABSTRACT *Listeria monocytogenes* is a foodborne bacterium that causes gastroenteritis, meningitis, or abortion. *Listeria* induces its internalization (entry) into some human cells through interaction of the bacterial surface protein InlB with its host receptor, the Met tyrosine kinase. InlB and Met promote entry through stimulation of localized actin polymerization and exocytosis. How actin cytoskeletal changes and exocytosis are controlled during entry is not well understood. Here, we demonstrate important roles for the host GTPase Arf1 and its effectors AP1 and PICK1 in actin polymerization and exocytosis during InlB-dependent uptake. Depletion of Arf1 by RNA interference (RNAi) or inhibition of Arf1 activity using a dominant-negative allele impaired InlB-dependent internalization, indicating an important role for Arf1 in this process. InlB stimulated an increase in the GTP-bound form of Arf1, demonstrating that this bacterial protein activates Arf1. RNAi and immunolocalization studies indicated that Arf1 controls exocytosis and actin polymerization during entry by recruiting the effectors AP1 and PICK1 to the plasma membrane. In turn, AP1 and PICK1 promoted plasma membrane translocation of both Filamin A (FlnA) and Exo70, two host proteins previously found to mediate exocytosis during InlB-dependent internalization (M. Bhalla, H. Van Ngo, G. C. Gyanwali, and K. Ireton, Infect Immun 87: e00689-18, 2018, https://doi.org/10.1128/IAI.00689-18). PICK1 mediated recruitment of Exo70 but not FlnA. Collectively, these results indicate that Arf1, AP1, and PICK1 stimulate exocytosis by redistributing FlnA and Exo70 to the plasma membrane. We propose that Arf1, AP1, and PICK1 are key coordinators of actin polymerization and exocytosis during infection of host cells by *Listeria*.

KEYWORDS AP1, Arf1, *Listeria monocytogenes*, PICK1, actin polymerization, exocytosis

The foodborne bacterium *Listeria monocytogenes* causes gastroenteritis, meningitis, or abortion (1). A critical aspect of *Listeria* virulence is the ability of bacteria to induce their internalization (entry) into nonphagocytic cells in the intestine, liver, or placenta (2). A major pathway of *Listeria* entry is mediated by binding of the bacterial surface protein InlB to its host receptor, the Met tyrosine kinase (3). InlB activates Met, resulting in the stimulation of two host processes that promote bacterial uptake: actin polymerization and exocytosis (4–7).

Actin polymerization is thought to contribute to uptake of *Listeria* by providing a protrusive force that pushes the plasma membrane around adherent bacteria (4, 8). Exocytosis is the fusion of intracellular vesicles with the plasma membrane (9). This process contributes to *Listeria* entry in part by redistributing the host GTPase Dynamin 2 (6). During InlB-mediated internalization, exocytosis mediates the translocation of Dynamin 2 from an internal membrane compartment, termed the recycling endosome (RE), to sites in the plasma membrane that underlie adherent bacteria. Importantly,

Citation Saila S, Gyanwali GC, Hussain M, Gianfelice A, Ireton K. 2020. The host GTPase Arf1 and its effectors AP1 and PICK1 stimulate actin polymerization and exocytosis to promote entry of *Listeria monocytogenes*. Infect Immun 88:e00578-19. https://doi.org/10.1128/IAI.00578-19.

Editor Nancy E. Freitag, University of Illinois at Chicago

Address correspondence to Keith Ireton, keith.ireton@otago.ac.nz.

Received 1 August 2019
Returned for modification 2 September 2019
Accepted 10 November 2019
Accepted manuscript posted online 18 November 2019
Published 22 January 2020

Dynamin 2 has a critical role in InlB-mediated internalization of *Listeria* (6, 10). Dynamin 2 can remodel membranes through a GTP-dependent scission activity and also by interacting with membrane-sculpting proteins containing BAR domains (11). It seems likely that these membrane-remodeling activities of Dynamin 2 are responsible for the ability of the GTPase to promote uptake of *Listeria*.

An important question is how actin polymerization and exocytosis are stimulated during InlB-mediated entry. The mechanisms of stimulation of these processes have been partly elucidated. Actin filament assembly during entry is mediated, at least in part, through the host Arp2/3 complex and upstream activators of this complex, including the nucleation-promoting factors N-WASP and WAVE and the small GTPases Cdc42 and Rac1 (5, 12–14). Although less is known about how exocytosis is stimulated during InlB-dependent uptake, recent results have shed some light on this topic. Upregulation of exocytosis during *Listeria* entry requires the tyrosine kinase activity of the Met receptor and a downstream host signaling pathway comprised of the serine/threonine kinases mTOR and protein kinase C-α (PKC-α) and the scaffolding protein Filamin A (FlnA) (7). mTOR affects exocytosis by mobilizing FlnA to the plasma membrane, whereas PKC-α phosphorylates FlnA on a serine residue located in a carboxyl-terminal immunoglobulin-like repeat. This phosphorylation event enhances the ability of FlnA to stimulate exocytosis. FlnA promotes exocytosis by recruiting a multicomponent complex, termed the exocyst. The exocyst is known to mediate polarized exocytosis by tethering exocytic vesicles to specific sites in the plasmalemma (15). Despite these recent advances, our understanding of regulatory mechanisms of actin polymerization and exocytosis during entry of *Listeria* is likely incomplete.

One group of mammalian proteins that has the potential to control actin filament assembly and exocytosis during uptake of *Listeria* is Arf family GTPases (16–18). Based on amino acid sequence, three classes of mammalian Arf proteins have been described (17). Class I Arf proteins (Arf1, Arf2, and Arf3) localize mainly to the Golgi apparatus but also function in the endosomal system. The best-characterized class I protein is Arf1, which controls multiple membrane trafficking events, including retrograde transport of vesicles from the *trans*-Golgi network (TGN) to the endoplasmic reticulum (ER), transport of TGN-derived vesicles to early and late endosomes, clathrin-independent endocytosis, and RE-mediated exocytosis (16–20). Interestingly, Arf1 also controls Arp2/3-dependent actin polymerization at the plasma membrane (18, 20, 21). Class II Arf proteins consist of Arf4 and Arf5 (16, 17). Overall, the functions of these two GTPases are not well understood. However, recent data indicate that Arf4 acts at the TGN to control vesicular transport of rhodopsin to cilia, Arf5 promotes endocytosis of integrin receptors, and Arf4 and Arf5 cooperate to stimulate exocytosis of dense core vesicles from nerve terminals (16, 22). The sole class III Arf protein is Arf6. This GTPase acts in endosomes and at the plasma membrane to regulate endocytosis, membrane recycling, and actin polymerization (16–18).

Arf GTPases are activated by binding to GTP (16, 17). The GTP-bound state of Arf proteins is increased or decreased by various guanine nucleotide exchange factors (GEFs) or GTPase-activating proteins (GAPs), respectively. When activated, Arf GTPases accomplish their biological activities by interacting with several effector proteins. For example, Arf1-GTP promotes transport of TGN-derived vesicles to early endosomes or the RE by binding the gamma subunit of the adaptor protein complex AP1 (23, 24). AP1 directs vesicular transport by recruiting specific cargo into clathrin-coated buds that emerge from the TGN. In addition to affecting membrane trafficking, activated Arf1 also controls Arp2/3-dependent actin polymerization at the plasma membrane by engaging the WAVE regulatory complex (WRC) (18), the BAR domain-containing protein PICK1 (21), or the lipid kinase phosphatidylinositol 4-phosphate 5-kinase (PIP5K1A) (25).

To date, the roles of Arf proteins in InlB-mediated entry of *Listeria* have not been comprehensively investigated. The only Arf protein previously examined for a function in *Listeria* uptake is Arf6. Interestingly, this GTPase limits InlB-mediated entry under conditions in which the GAP ARAP2 is depleted by RNA interference (RNAi) (26). In contrast, when ARAP2 expression is normal, Arf6 has no detectable role in InlB-

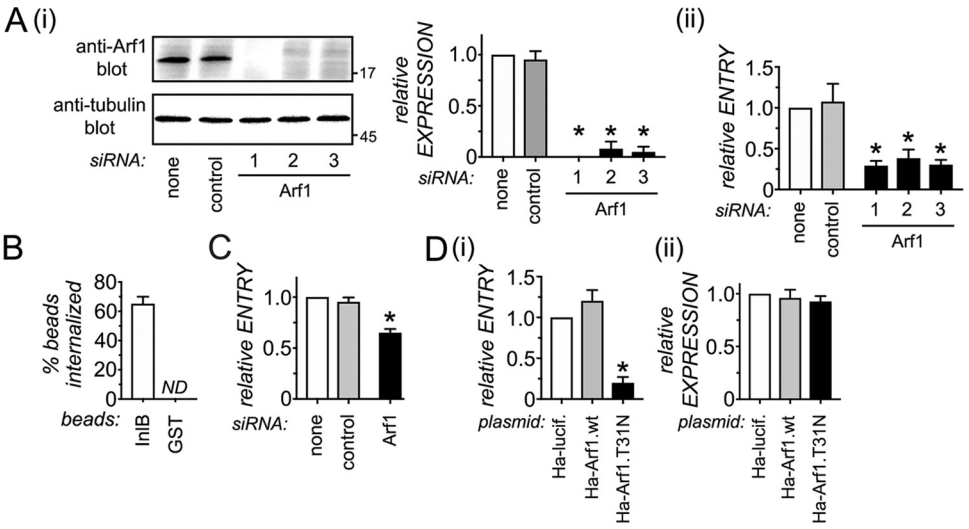

FIG 1 Host Arf1 promotes InlB-mediated entry. (A) Effect of siRNAs against Arf1 on target protein expression and entry of *Listeria*. HeLa cells were mock transfected in the absence of siRNA, transfected with a control nontargeting siRNA, or transfected with three different siRNAs against Arf1. Cells were then solubilized for analysis of target gene expression by Western blotting (i) or infected with *Listeria* for assessment of entry by gentamicin protection assays (ii). (B) Internalization of InlB-coated beads. HeLa cells were incubated with beads coated with InlB or GST for 30 min, followed by fixation, labeling, and quantification of bead internalization, as described in Materials and Methods. Results are means ± SEM from three experiments. In each experiment, approximately 200 cell-associated beads coated with InlB or 50 beads associated with GST were analyzed for entry. *, $P < 0.05$ compared to the control siRNA condition. (C) Inhibition of entry of InlB-coated beads by an siRNA targeting Arf1. The results are means ± SEM from three experiments. In each experiment, approximately 100 cell-associated beads were scored for each condition. *, $P < 0.05$ compared to the control siRNA condition. (D) Effect of Arf1.T31N on internalization of InlB-coated particles. HeLa cells transiently expressing HA-tagged wild-type (wt) Arf1, Arf1.T31N, or luciferase as a control were incubated with InlB-coated beads for 30 min, followed by fixation, labeling, and analysis of bead internalization. The data are means ± SEM from four experiments. *, $P < 0.05$ compared to HA-Arf1.wt.

dependent entry. Since ARAP2 normally inactivates Arf6 by stimulating GTP hydrolysis (27), these findings indicate that unrestrained activation of Arf6 impairs internalization of *Listeria*. The roles of the remaining four human Arf proteins (Arf1, Arf3, Arf4, and Arf5) in internalization of *Listeria* remain to be addressed. In this regard, it is worth noting that human cells lack Arf2, an Arf protein present only in mice (16).

In this work, we examined the roles of Arf1, Arf3, Arf4, and Arf5 in entry of *Listeria* into the human cell line HeLa. Our findings demonstrate an important function for Arf1 in controlling actin polymerization and exocytosis during InlB-dependent uptake. Genetic, biochemical, and microscopy-based studies indicate that Arf1 is activated by InlB and promotes actin polymerization and exocytosis through recruitment of the effectors AP1 and PICK1. We also present evidence that AP1 and PICK1 control exocytosis during InlB-mediated entry by mediating translocation of FlnA and Exo70 to the plasma membrane. Collectively, our findings identify Arf1 and its effectors AP1 and PICK1 as important coordinators of actin polymerization and exocytosis during infection of host cells by *Listeria*.

RESULTS

The host GTPase Arf1 promotes InlB-mediated entry of *Listeria*. RNA interference (RNAi) was used to investigate the functions of Arf1, Arf3, Arf4, and Arf5 in entry of *Listeria* into the human cell line HeLa. Previous findings indicated that internalization into HeLa cells is dependent on InlB but not on other bacterial factors (26, 28, 29). Short interfering RNAs (siRNAs) were transfected into HeLa cells to deplete various Arf proteins. In order to control for potential off-target effects (30), three siRNAs were used to target each GTPase. As controls, cells were mock transfected in the absence of siRNA or transfected with a control nontargeting siRNA that lacks complementarity to any known human mRNA. In the case of Arf1, depletion of the target protein by siRNAs was confirmed by Western blotting (Fig. 1A). For the remaining Arf proteins, quantitative

PCR (qPCR) was used to verify knockdown at the mRNA level, since effective antibodies were not commercially available (see Fig. S1 in the supplemental material). siRNAs targeting Arf1 caused a greater than 90% depletion of Arf1 protein and a 60 to 70% inhibition in entry of *Listeria* (Fig. 1A). siRNAs against Arf3, Arf4, or Arf5 decreased target mRNA expression by 75 to 95%, indicating that the corresponding GTPases were substantially depleted (Fig. S1). However, siRNAs against these three Arf proteins generally caused less severe inhibition in entry of *Listeria* than the Arf1 siRNAs. For this reason, and because Arf1 is better characterized than the other Arf proteins, we decided to focus the remainder of our study on Arf1.

In order to strengthen the evidence for a role for Arf1 in InlB-dependent entry, we next determined the effect of inhibition of Arf1 on uptake of inert particles coated with InlB. Latex beads (3 μm in diameter) have been extensively used as a model for InlB-dependent entry, since these particles lack other bacterial factors and are efficiently internalized into mammalian cells in a manner that depends on the Met receptor and other host proteins involved in *Listeria* uptake (6, 12, 13, 26, 29, 31–34). As previously reported (6, 7, 29, 34, 35), beads coupled to InlB were efficiently internalized into HeLa cells, whereas control beads coupled to glutathione *S*-transferase (GST) were not internalized (Fig. 1B). The siRNA against Arf1 that caused the largest inhibition in entry of *Listeria* next was used to deplete Arf1, and the effect on uptake of InlB-coated beads was assessed. Internalization of beads was inhibited by about 40% (Fig. 1C). Collectively, the results shown in Fig. 1A to C indicate an important role for Arf1 in InlB-dependent entry.

InlB-dependent entry involves the activated form of Arf1. We used a dominant-negative allele of Arf1 to determine if InlB-mediated entry requires Arf1-GTP. Arf1 containing a threonine-to-asparagine substitution at residue 31 (T31N) has been extensively used as a tool to inhibit Arf1 activity in mammalian cells (16, 36–41). When overexpressed, this Arf1.T31N protein is thought to inhibit activation of endogenous Arf1 by sequestering GEFs that would otherwise stimulate GTP loading on the endogenous protein (16). HeLa cells were transiently transfected with plasmids expressing hemagglutinin (HA) epitope-tagged Arf1.T31N or HA-tagged wild-type Arf1 (Arf1.wt). As a control, cells were transfected with a plasmid expressing HA-tagged luciferase, which does not affect InlB-dependent entry (34). Cells were then incubated with InlB-coated beads for 30 min, and entry of particles was assessed using a previously described fluorescence microscopy-based approach (7, 26, 29, 34, 35). Internalization of InlB-coated beads was inhibited by ~80% in cells expressing tagged Arf1.T31N compared to cells expressing tagged Arf1.wt (Fig. 1D). These findings suggest an important role for the GTP-bound form of Arf1 in InlB-dependent entry. We note that the inhibition in InlB-dependent entry caused by Ha.Arf1.T31N was greater than the ~40% decrease in internalization resulting from RNAi-mediated depletion of Arf1 (Fig. 1C). Some Arf1 GEFs also control other Arf GTPases, including Arf3 and Arf5 (42). Because Arf3 and Arf5 may participate in InlB-mediated entry (Fig. S1), it is possible that the effects of Arf1.T31N on entry are due to combined inhibition of Arf1, Arf3, and Arf5.

The results shown in Fig. 1D suggest that InlB induces an increase in cellular levels of Arf1-GTP. To test this idea, we used a previously described approach involving coprecipitation of Arf1-GTP with its effector, GGA3 (40, 43–45). Before proceeding with the studies with InlB, we confirmed that the coprecipitation technique selectively detects Arf1-GTP in HeLa cells. As expected, Arf1 was present in GGA3 precipitates prepared from lysates loaded with the nonhydrolyzable GTP analog GTP-gamma S but not in precipitates of lysates loaded with GDP (Fig. 2A). In addition, HA-tagged wild-type Arf1 (Arf1.wt) or a constitutively activated form of Arf1 (Arf1.Q71L) coprecipitated with GGA3, whereas tagged Arf1.T31N failed to coprecipitate (Fig. 2B). Having validated the Arf1 activation assay, we next determined if InlB activates Arf1 by treating HeLa cells with soluble InlB protein. When used at low-nanomolar concentrations, soluble InlB is a potent agonist of the Met receptor and its associated downstream signaling pathways (3, 7, 29, 34, 46, 47). HeLa cells were either left untreated or treated

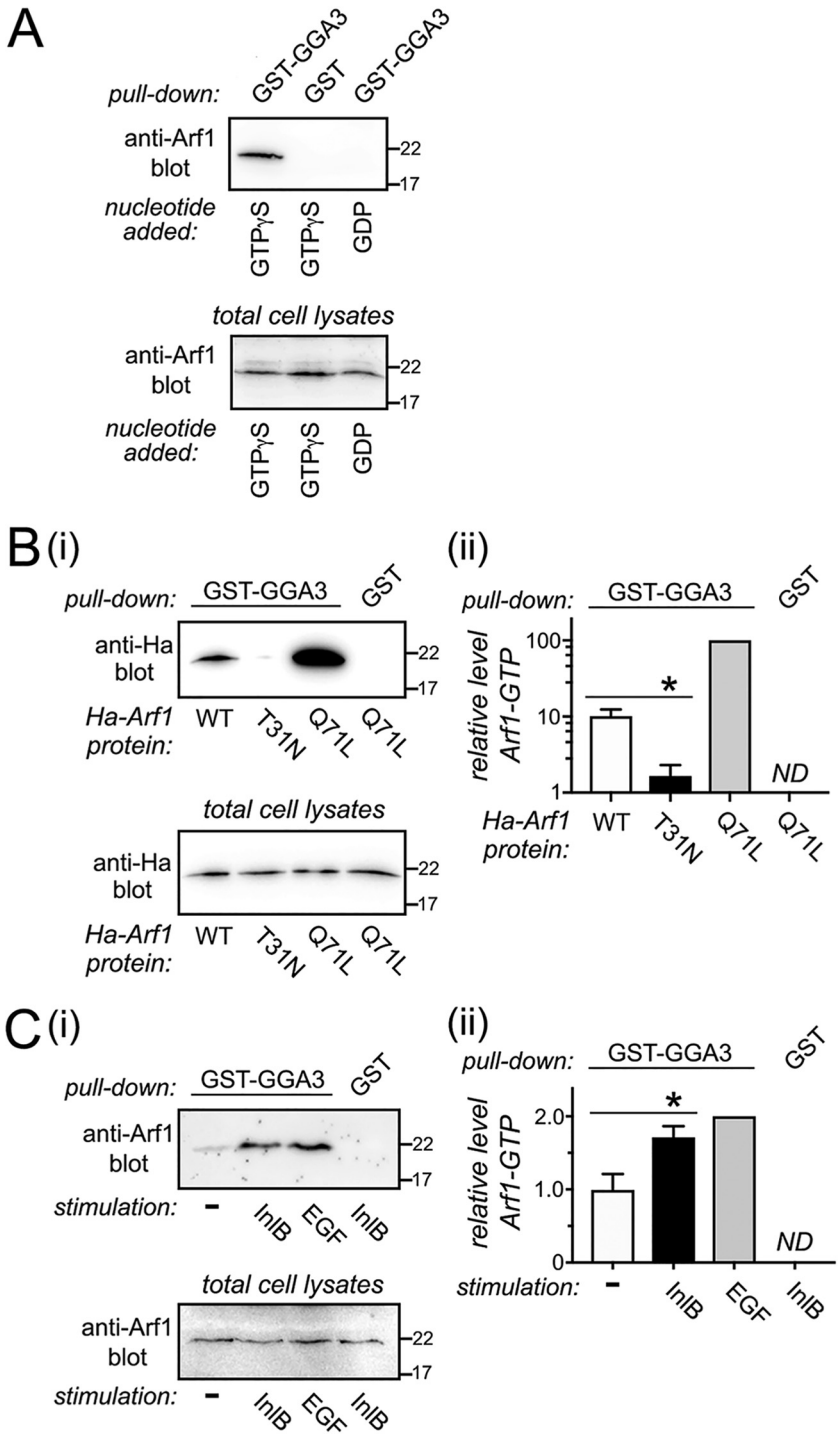

FIG 2 InlB induces an increase in Arf1-GTP levels. (A) Validation of the GST-GGA3 pulldown assay to measure Arf1-GTP. Lysates of HeLa cells were incubated in the absence of nucleotide, with GTPγS, or with GDP for 30 min, followed by precipitation with GST-GGA3 or GST. Arf1-GTP in precipitates was detected by Western blotting. Total cell lysates used for the precipitations were also Western blotted with anti-Arf1 antibodies to confirm similar levels of Arf1. Representative blots are shown. The experiment was performed three times, with similar results. (B) Ability of wild-type and mutant forms of Arf1 to interact with GST-GGA3. HeLa cells transiently expressing HA-tagged Arf1 wild type (WT), Arf1.T31N, or Arf1.Q71L were solubilized, and lysates were used for pulldowns with GST-GGA3 or GST. Precipitates or total cell lysates were Western blotted with anti-HA antibodies. (i) Western blots from a representative experiment are shown. (ii) Quantified Western blotting data from three experiments are provided. To obtain relative Arf1-GTP levels, data were normalized to those of Arf1.Q71L. ND, not detected. *, $P < 0.05$. (C) Stimulation of Arf1 activity by InlB. HeLa cells were either left untreated (−) or treated with soluble InlB or EGF for 5 min. Lysates were used for pulldowns with GST-GGA3 or GST. (i) Representative anti-Arf1 Western blots

(Continued on next page)

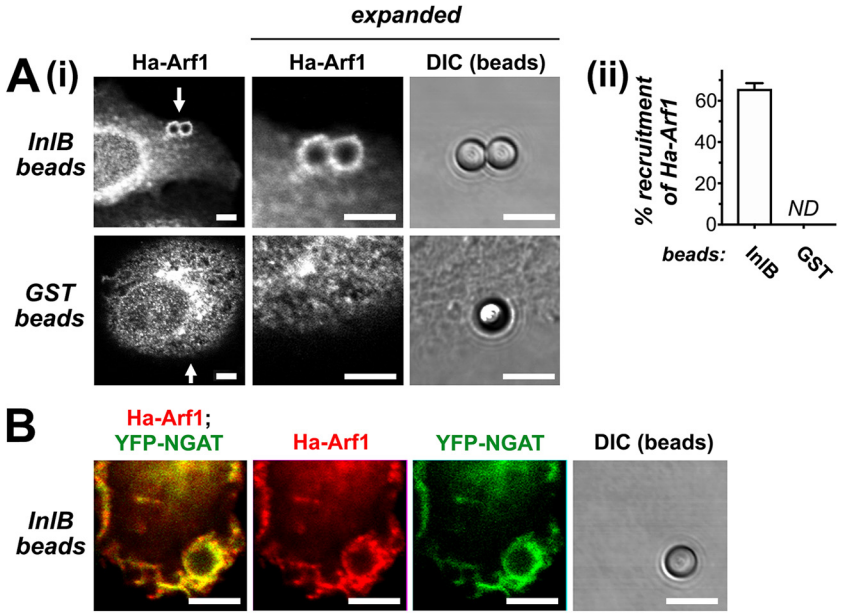

FIG 3 Arf1 is recruited during internalization of InlB-coated particles. (A) Accumulation of Arf1 around InlB-coated beads. HeLa cells transiently expressing HA-tagged wild-type Arf1 were incubated with beads coated with InlB or GST for 5 min, followed by fixation, labeling, and imaging by confocal microscopy. (i) Representative images of HA-Arf1 localization are shown. Panels on the left display HA-Arf1 distribution, with locations of beads indicated with arrows. Regions near beads are expanded in the middle and right panels. Middle panels show HA-Arf1 labeling, whereas right panels are differential interference contrast (DIC) images displaying beads. Scale bars indicate 5 μm. (ii) Data showing the percentage of cell-associated beads that recruited HA-Arf1. ND indicates that no intracellular beads coated with GST were detected. Results are means ± SEM from three experiments. In each experiment, approximately 100 cell-associated beads were scored for recruitment. (B) Corecruitment of Arf1 and NGAT around InlB-coated particles. HeLa cells transiently coexpressing HA-Arf1 and YFP-NGAT were incubated with InlB-coated beads for 5 min, followed by fixation and labeling of HA-Arf1. A representative confocal microscopy image is presented. Scale bars indicate 5 μm. Analysis from three experiments indicated that 65.8% ± 2.3% (standard deviations) of beads that recruited Arf1 also recruited YFP-NGAT. In each experiment, approximately 150 beads were analyzed.

with 4.5 nM soluble InlB for 5 min. As a positive control, cells were incubated for 5 min with 15 nM epidermal growth factor (EGF), a known activator of Arf1 (44, 45). Importantly, compared to untreated conditions, treatment with InlB caused an ~70% increase in Arf1-GTP levels (Fig. 2C), indicating that InlB activates Arf1.

Arf1 redistributes to the plasma membrane during InlB-mediated entry. Although Arf1 is present predominantly in the Golgi apparatus in the absence of cell stimulation (16), a subcellular pool of this GTPase redistributes to the plasmalemma during endocytosis or phagocytosis (16, 37–39, 48). Importantly, we found that HA-tagged Arf1 localized in ring-like structures around InlB-coated beads that were incubated with HeLa cells for 5 min (Fig. 3A). In contrast, Ha-Arf1 failed to localize around beads coated with GST (Fig. 3A), which are not internalized into host cells (Fig. 1B). We next examined if HA-Arf1 accumulating around InlB-coated beads colocalizes with a marker of Arf1 activation. For this purpose, we used a probe consisting of yellow fluorescent protein (YFP) fused to the N-terminal GAT domain of the Arf1 effector GGA1. This YFP-NGAT probe was previously used to demonstrate activation of Arf1 during Fcγ receptor-mediated phagocytosis in macrophages (37). Importantly, ~66% of InlB-coated beads that induced accumulation of Ha-Arf1 also displayed recruitment

FIG 2 Legend (Continued)
of precipitates (top) or total cell lysates (bottom) are shown. (ii) Quantified Western blotting data for Arf1-GTP from six experiments are provided. Data are means ± SEM. *, $P < 0.05$ compared to the control siRNA condition.

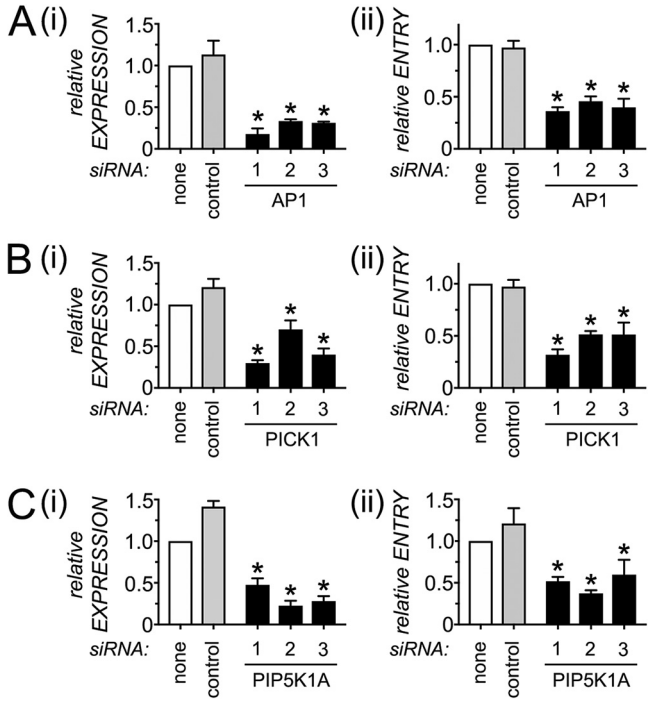

FIG 4 Arf1 effectors AP1, PICK1, and PIP5K1A are needed for efficient entry of *Listeria*. HeLa cells were mock transfected in the absence of siRNA, transfected with a control nontargeting siRNA, or transfected with three different siRNAs against AP1 (A), PICK1 (B), or PIP5K1A (C). Cells were then solubilized for measurement of target gene expression by qPCR (i) or infected with *Listeria* for evaluation of entry (ii). Entry or expression data are means ± SEM from three to eight experiments, depending on the condition. *, $P < 0.05$ compared to the control siRNA condition.

of YFP-NGAT (Fig. 3B). Collectively, the data shown in Fig. 3 suggest that activated Arf1 is recruited to sites of InlB-mediated entry.

The Arf1 effectors AP1, PICK1, and PIP5K1A contribute to InlB-dependent uptake. The role of Arf1-GTP in InlB-mediated internalization and the ability of InlB to activate Arf1 (Fig. 1D, 2C, and 3B) suggested that Arf1 affects uptake of *Listeria* through one or more effector proteins. We used RNAi to examine if InlB-mediated entry involves three known Arf1 effectors: the gamma subunit of the adaptor protein AP1, the BAR domain-containing protein PICK1, and the lipid kinase type IA alpha phosphatidylinositol 4-phosphate 5 kinase (PIP5K1A) (16, 21, 23–25, 49). In these experiments, siRNA-mediated inhibition in expression of PICK or PIP5K1A was confirmed by qPCR, since effective commercially available antibodies against these proteins were unavailable (Fig. 4). In the case of AP1, both qPCR and Western blotting were used to assess reduction in target gene expression (Fig. 4 and Fig. S2). Importantly, these RNAi-based experiments demonstrated that each of the three Arf1 effectors contributes to internalization of *Listeria* (Fig. 4) and InlB-coated beads (Fig. S3).

We next examined if AP1 or PICK1 was recruited to the plasma membrane during InlB-mediated entry. We were unable to examine recruitment of PIP5K1A, as effective antibodies or constructs expressing tagged PIP5K1A were not available. Importantly, AP1 and PICK1 each accumulated around InlB-coated beads that were in the process of entering into HeLa cells (Fig. 5, no siRNA condition). In contrast, these two Arf1 effectors failed to be recruited around control beads coated with GST. We next investigated if Arf1 acts upstream of AP1 and PICK1 to recruit these effectors to the plasma membrane during entry. Importantly, treatment of HeLa cells with an siRNA targeting Arf1 inhibited accumulation of AP1 or PICK1 around InlB-coated beads (Fig. 5A and B). Specifically, the proportion of InlB-coated particles that recruited AP1 or PICK1 was reduced by 70 or 62%, respectively (Fig. 5C). These results indicate that Arf1 modulates these

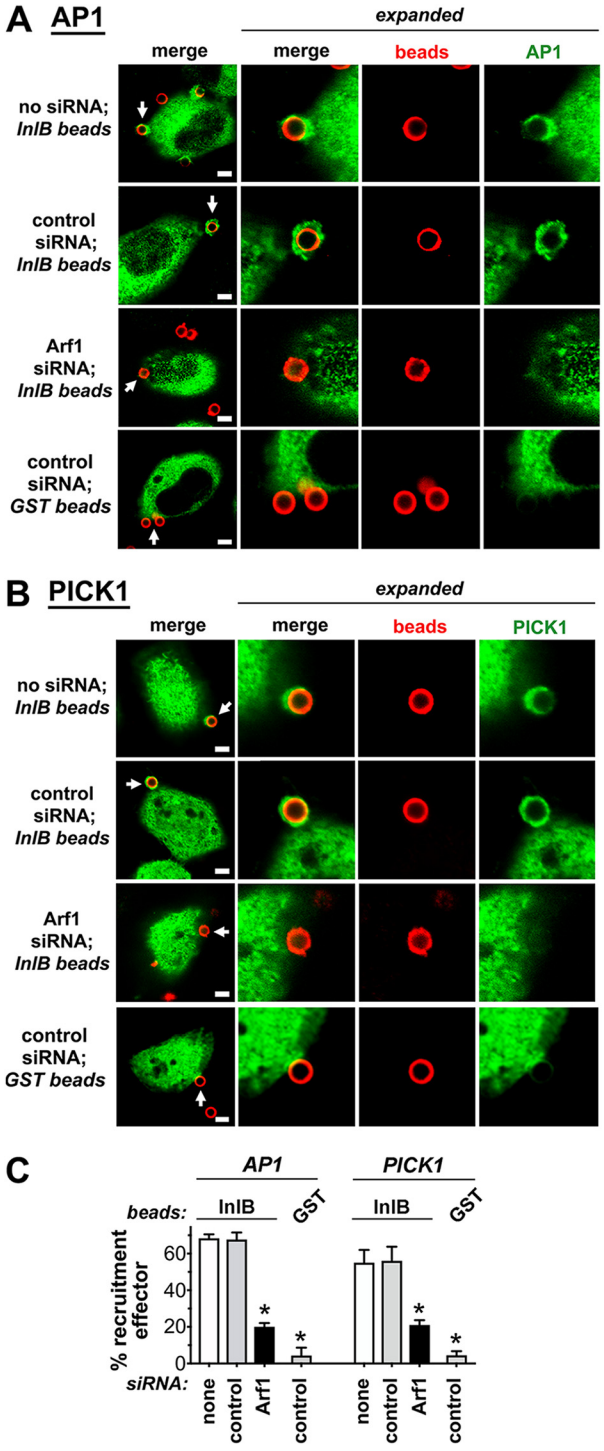

FIG 5 Arf1 mediates recruitment of AP1, PICK1, and PIP5K1A during InlB-dependent entry. HeLa cells were subjected to control conditions or transfected with an siRNA targeting Arf1. About 24 h later, cells were transfected with plasmids transiently expressing HA-tagged AP1 or myc-tagged PICK1. HeLa cells were then incubated with beads coupled to InlB or GST for 5 min, followed by fixation, labeling, and imaging by confocal microscopy. (A and B) Representative images of recruitment of AP1 or PICK1 are shown. Areas near beads indicated with arrows in the left panels are expanded in the middle and right panels. Scale bars represent 5 μm. (C) Quantification of effects of Arf1 RNAi on recruitment of effectors. Data are means ± SEM from three experiments. In each experiment, 30 to 80 cell-associated beads were scored for each condition. *, $P < 0.05$ compared to the no siRNA or control siRNA conditions for InlB-coated beads.

effectors, at least in part, by promoting their redistribution to the plasma membrane during InlB-mediated uptake.

Arf1 and AP1 do not affect surface levels of the Met receptor. Because Arf1 and AP1 are known to promote postendocytic recycling of transmembrane proteins (16, 17, 23), we considered the possibility that these two host proteins affect InlB-dependent entry by controlling surface levels of the Met receptor. In order to test this idea, Arf1 or AP1 was depleted by RNAi, and surface Met was detected using an established method involving biotinylation of surface proteins (6, 50, 51). As a positive control predicted to affect Met surface levels, Met was knocked down by RNAi. Importantly, RNAi-mediated depletion of Arf1 or AP1 failed to reduce the amount of Met receptor on the surface of HeLa cells (Fig. S4). These results indicate that Arf1 and AP1 do not have appreciable roles in maintaining surface levels of Met and instead control InlB-mediated entry by acting downstream of this host receptor.

Arf1 and its effectors promote actin polymerization and exocytosis during entry. Previous findings indicate that F-actin accumulates in cup-like structures around InlB-coated beads that are being internalized into host cells (6, 26, 29, 34). In addition, entry of InlB-coated beads is inhibited by treatment of HeLa cells with the actin polymerization inhibitor cytochalasin D (29) or by genetic inhibition of the Arp2/3 complex (5, 12, 13, 35). These results demonstrate that InlB-dependent uptake requires local stimulation of actin polymerization at sites of entry. We used RNAi to investigate the role of Arf1 and its effectors in actin filament assembly during InlB-dependent uptake. HeLa cells were treated with siRNAs targeting Arf1, the gamma subunit of AP1, PICK1, or PIP5K1A. As negative controls, cells were mock transfected in the absence of siRNA or transfected with control siRNA. As a positive control expected to inhibit actin polymerization during entry, cells were treated with an siRNA against Met (6, 7, 26, 29, 34). Transfected cells then were incubated for 5 min with InlB-coated beads or with GST-coated beads as a control. Samples were fixed, labeled for filamentous (F)-actin and extracellular beads, and imaged by confocal microscopy. In order to quantify effects of Arf1 depletion on actin polymerization, we measured the degree of accumulation of F-actin around InlB-coated beads using fold enrichment (FE) values, as described previously (6, 7, 26, 34, 35). FE is defined as the mean fluorescence intensity of a host protein around beads normalized to the mean fluorescence intensity of the protein throughout the human cell. An FE value greater than 1.0 indicates enrichment of the host protein around particles. As previously reported (6, 7, 26, 34, 35), F-actin accumulated around InlB-coated beads in HeLa cells that were mock transfected in the absence of siRNA or treated with a control siRNA (Fig. 6A). The mean FE values for F-actin under these conditions were 1.7 and 1.6, respectively, demonstrating enrichment of F-actin around InlB-coated particles (Fig. 6B). In contrast, F-actin failed to accumulate around GST-coated beads (Fig. 6A), as indicated by a mean FE value of less than 1.0 (Fig. 6B). Importantly, RNAi-mediated knockdown of Arf1, AP1, PICK1, PIP5K1A, or Met each decreased accumulation of F-actin around InlB-coated beads (Fig. 6A), resulting in mean FE values between 1.2 and 1.4. Taken together, these results demonstrate that Arf1, AP1, PICK1, and PIP5K1A are needed for actin cytoskeletal changes that accompany InlB-mediated uptake.

In order to determine the role of Arf1 and its effectors in exocytosis during entry, we used a probe consisting of the v-SNARE protein VAMP3 fused to green fluorescent protein (VAMP3-GFP) (6, 7, 52). Prior to exocytosis, VAMP3-GFP resides in intracellular vesicles derived from the RE. When vesicles fuse with the plasma membrane during exocytosis, the GFP moiety becomes extracellular (exofacial) and can be labeled with antibodies without cell permeabilization. HeLa cells were subjected to control conditions or transfected with siRNAs against Arf1, its effectors, or Met. After siRNA transfection, cells were transfected with a plasmid expressing VAMP3-GFP, incubated with beads coated with InlB or GST, fixed, and labeled for exofacial VAMP3-GFP, as described previously (6, 7, 52). Confocal microscopy images were acquired to quantify FE values

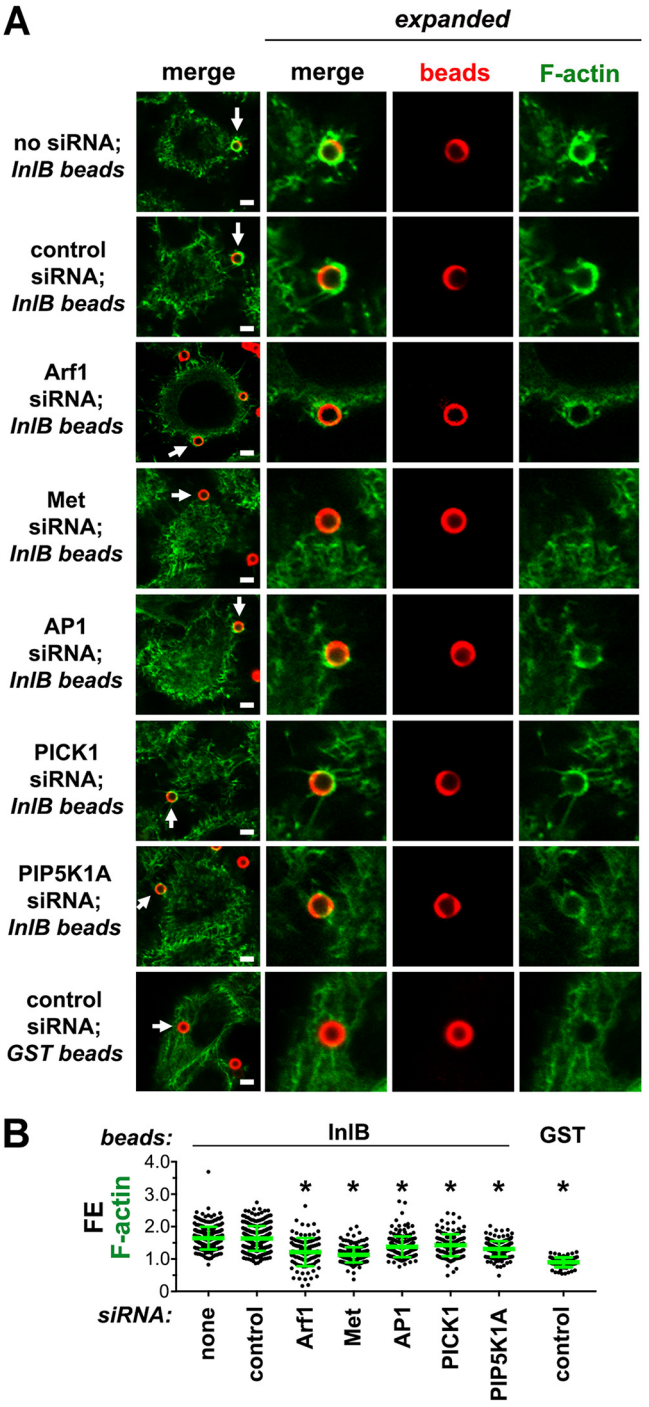

FIG 6 Arf1 and its effectors promote actin polymerization during InlB-mediated uptake. HeLa cells were subjected to control conditions or transfected with siRNAs against Arf1, Met, AP1, PICK1, or PIP5K1A and then incubated with beads coated with InlB or GST for 5 min. Samples were fixed, labeled, and imaged by confocal microscopy. (A) Representative images are presented. Regions near beads indicated with arrows in the left panels are expanded in the middle and right panels. Scale bars indicate 5 μm. (B) Fold enrichment (FE) values for F-actin are shown. Each dot represents an FE measurement for an individual bead. Data are pooled FE values from three experiments. In each experiment, approximately 60 extracellular, cell-associated beads were analyzed for each condition. *, $P < 0.05$ compared to the no siRNA or control siRNA conditions for InlB-coated beads.

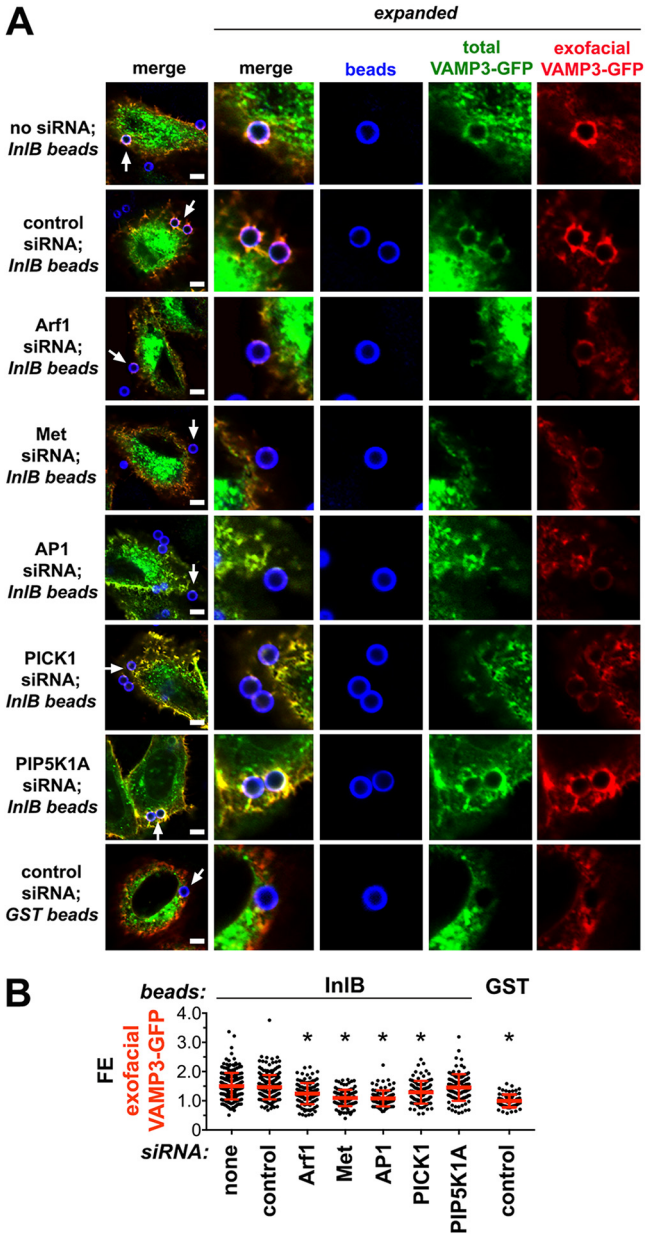

FIG 7 Arf1 and its effectors control exocytosis during InlB-dependent entry. HeLa cells were either subjected to control conditions or transfected with siRNAs targeting Arf1, Met, AP1, PICK1, or PIP5K1A. Cells were then incubated with particles coupled to InlB or GST for 5 min, fixed, labeled, and imaged by confocal microscopy. (A) Representative images are shown. Regions near beads indicated with arrows in the left panels are expanded in the middle and right panels. Scale bars represent 5 μm. (B) FE values for exofacial VAMP3-GFP are presented. Data are pooled FE values from three experiments. In each experiment, approximately 40 extracellular, cell-associated beads were analyzed for each condition. *, $P < 0.05$ compared to the no siRNA or control siRNA conditions for InlB-coated beads.

for exofacial VAMP3-GFP, as detailed earlier (6, 7). The results indicate that siRNAs against Arf1, AP1, PICK1, and Met each decreased exocytosis around InlB-coated particles (Fig. 7). In contrast, depletion of PIP5K1A failed to affect exocytosis. Collectively, the results shown in Fig. 7 demonstrate important functions for Arf1 and its effectors AP1 and PICK1 in exocytosis during InlB-mediated entry.

Arf1 and AP1 recruit FlnA and the exocyst complex during entry. Previous findings indicate that exocytosis during InlB-mediated internalization is controlled by the exocyst complex and the scaffolding protein Filamin A (FlnA) (7). The exocyst is an

8-protein complex that promotes polarized exocytosis by tethering RE-derived vesicles to the plasma membrane in a step that precedes vesicle-plasma membrane fusion (15). During entry of InlB-coated beads, multiple exocyst components, including Exo70, are recruited to the plasma membrane (7). Importantly, recruitment of the exocyst component Exo70 during entry requires FlnA. Finally, RNAi-based experiments demonstrate that FlnA and the exocyst complex mediate exocytosis during uptake of InlB-coated particles.

We investigated if Arf1 and its effectors promote exocytosis during entry through recruitment of FlnA and/or the exocyst. RNAi was used to deplete Arf1, AP1, PICK1, PIP5K1A, or Met in HeLa cells, and the resulting effects on accumulation of FlnA or Exo70 around InlB-coated beads were assessed. Importantly, siRNAs targeting Arf1, AP1, or Met each inhibited recruitment of endogenous FlnA (Fig. 8) or enhanced GFP (EGFP)-tagged Exo70 (Fig. 9). In contrast, an siRNA against PI5P5K1A failed to reduce accumulation of FlnA or EGFP-Exo70 around InlB-coated beads. Interestingly, an siRNA targeting PICK1 impaired recruitment of EGFP-Exo70 but augmented recruitment of FlnA. These findings indicate that Arf1 and its effector, AP1, promote exocytosis during InlB-mediated entry through recruitment of both FlnA and the exocyst complex. In contrast, PICK1 likely affects exocytosis through mobilization of Exo70 alone. The different requirements for AP1 and PICK1 in recruitment of FlnA imply that FlnA is not sufficient to mobilize the exocyst during entry.

Arf1 and AP1 redistribute from the RE to the plasma membrane during InlB-mediated entry. We further investigated the mechanisms of recruitment of Arf1, AP1, PICK1, FlnA, and Exo70 during InlB-dependent internalization. Arf1 and AP1 are known to localize to the RE as well as to the TGN (19, 23, 38, 53–55). Consistent with these reports, we found that in resting HeLa cells not stimulated with InlB, Arf1 and AP1 partly colocalized with VAMP3 (Fig. S5), a marker for the RE (9, 54, 55). In contrast, PICK1, FlnA, or Exo70 did not colocalize with VAMP3-GFP under these conditions. Importantly, when HeLa cells were incubated with InlB-coated beads, Arf1, AP1, PICK1, FlnA, and Exo70 each coaccumulated with VAMP3-GFP around these particles (Fig. 10). Taken together, the results shown in Fig. 10 and Fig. S5 suggest that Arf1 and AP1 use RE-mediated exocytosis to translocate from endomembranes to the plasma membrane during entry of InlB-coated beads. In contrast, recruitment of FlnA and Exo70 to the plasma membrane probably does not directly involve the RE but instead is likely mediated by Arf1 after this GTPase translocates to the plasmalemma.

We performed experiments to directly test the idea that Arf1 and AP1 transit to the plasma membrane through RE-mediated exocytosis. RE-mediated exocytosis induced by InlB-coated beads requires the v-SNARE VAMP3 and the t-SNARE Syntaxin 4 (Stx4) (6). We used RNAi to deplete VAMP3 or Stx4 and determined the resulting effects on accumulation of HA-tagged Arf1 or endogenous AP1 around InlB-coated particles. The results indicate that depletion of VAMP3 or Stx4 inhibited recruitment of Arf1 or AP1 around beads (Fig. 11). Collectively, the data shown in Fig. S5 and Fig. 10 and 11 support the idea that exocytosis redistributes Arf1 and AP1 from the RE to the plasma membrane during InlB-mediated entry.

DISCUSSION

Results in this work demonstrate important regulatory roles for Arf1 and its effectors AP1 and PICK1 in exocytosis during InlB-dependent internalization. Specifically, we found that these effectors promote exocytosis by recruiting the scaffolding protein FlnA and the exocyst component Exo70, two host factors previously shown to mediate exocytosis during uptake of *Listeria* (7).

In order to direct recruitment of FlnA and the exocyst complex to sites of InlB-mediated entry, Arf1 and its effectors must themselves translocate to the plasma membrane. Interestingly, our results suggest that translocation of Arf1 and AP1 involves exocytic delivery through the RE. Subcellular pools of Arf1 and AP1 localize to the RE in unstimulated HeLa cells. During InlB-dependent entry, Arf1 and AP1 redis-

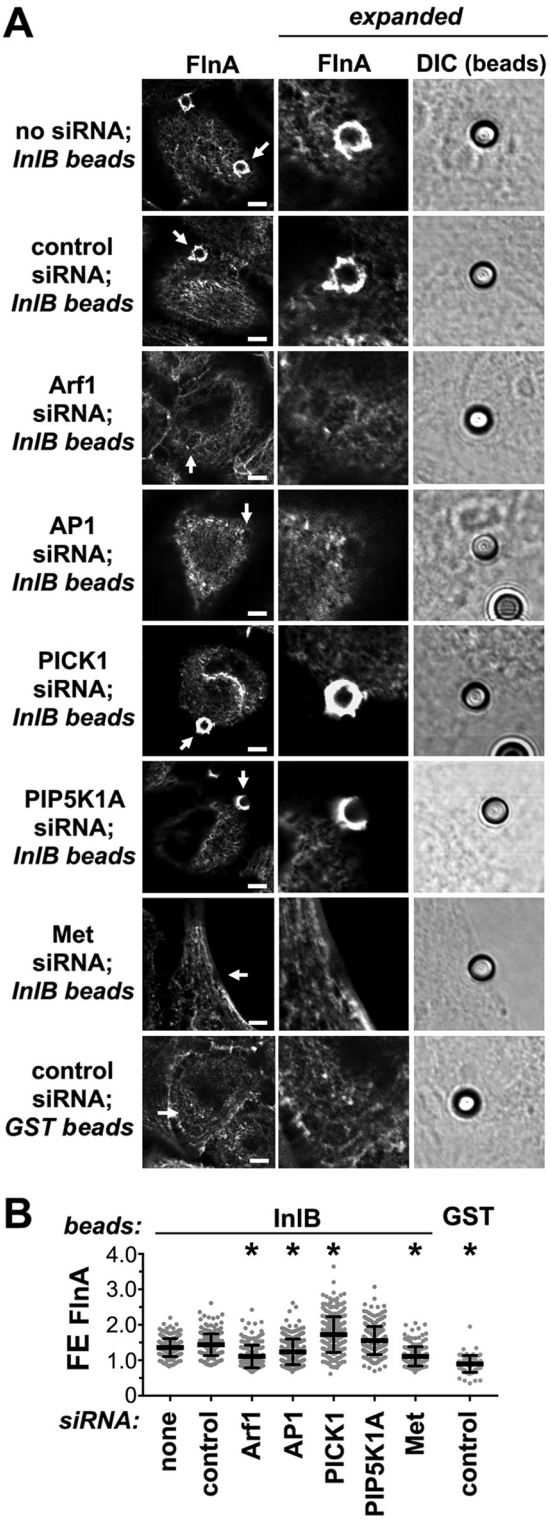

FIG 8 Arf1 and AP1 promote recruitment of the scaffolding protein FlnA. HeLa cells were mock transfected in the absence of siRNA, transfected with a control siRNA, or transfected with siRNAs against Arf1, AP1, PICK1, PIP5K1A, or Met. Cells were then incubated with InlB- or GST-coated beads for 5 min, fixed, labeled, and imaged by confocal microscopy. (A) Representative images are presented. Regions near beads indicated with arrows in the left panels are expanded in the middle and right panels. DIC indicates differential interference contrast images. Scale bars represent 5 μm. (B) Pooled FE values for FlnA from three experiments are presented. In each experiment, approximately 80 extracellular, cell-associated beads were analyzed for each condition. *, $P < 0.05$ compared to the no siRNA or control siRNA conditions for InlB-coated beads.

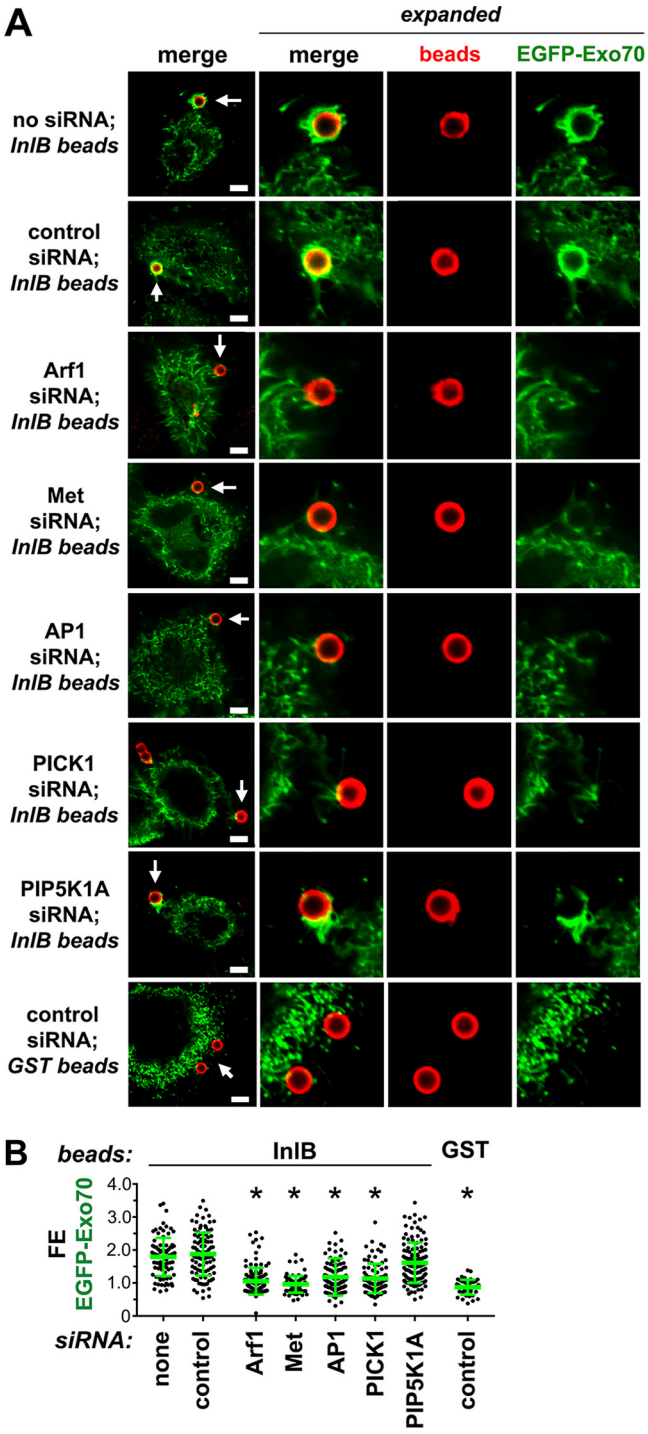

FIG 9 Arf1, AP1, and PICK1 mediate recruitment of Exo70 during InlB-dependent entry. After mock transfection or transfection with the indicated siRNAs, HeLa cells were transfected again with a plasmid expressing EGFP-Exo70. Cells were then incubated with InlB- or GST-coated particles for 5 min, fixed, labeled, and imaged by confocal microscopy. (A) Representative images are shown. Arrows indicate regions with beads that are enlarged in the middle and right panels. Scale bars represent 5 μm. (B) Pooled FE values for EGFP-Exo70 from three experiments are presented. In each experiment, approximately 40 extracellular, cell-associated beads were analyzed for each condition. *, $P < 0.05$ compared to the no siRNA or control siRNA conditions for InlB-coated beads.

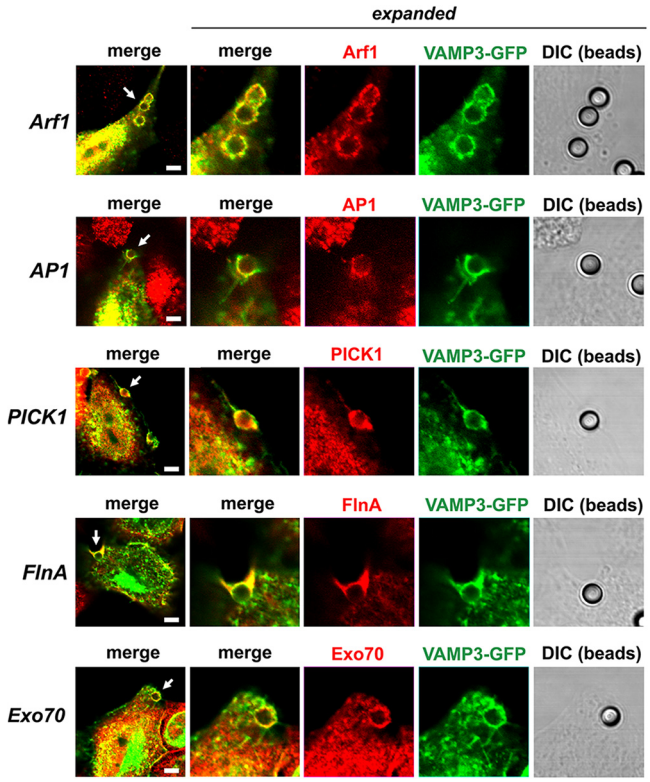

FIG 10 Arf1, AP1, PICK1, FlnA, and Exo70 are corecruited with VAMP3 during InlB-dependent internalization. HeLa cells transiently expressing VAMP3-GFP were incubated with InlB-coated beads for 5 min, fixed, and labeled for HA-tagged Arf1, myc-tagged PICK1, or endogenous AP1, FlnA, or Exo70. Representative confocal microscopy images are presented. Regions near beads indicated with arrows in the left panels are expanded in the middle and right panels. DIC indicates differential interference contrast images. Scale bars represent 5 μm. Yellow areas in the merged images represent colocalization of VAMP3-GFP with Arf1, AP1, PICK1, FlnA, or Exo70.

tribute to the plasma membrane, where they colocalize with VAMP3 around InlB-coated particles. This redistribution of Arf1 and AP1 is blocked by knockdown of VAMP3 or Stx4, conditions known to impair RE-mediated exocytosis (6). The lack of colocalization of FlnA and Exo70 with VAMP3 at endomembranes suggests that FlnA and Exo70 are absent from the RE. Nonetheless, accumulation of FlnA or Exo70 around InlB-coated beads is dependent on Arf1 and AP1. Collectively, our results suggest a mechanism of translocation of FlnA during InlB-dependent entry that involves exocytic trafficking of Arf1 and AP1 to the plasma membrane, followed by Arf1- and AP1-dependent recruitment of FlnA. FlnA, in turn, recruits Exo70 (7). At present, it remains unclear whether Arf1 directly mobilizes FlnA through physical interaction or whether Arf1 has a less direct role in recruitment.

Like AP1, the Arf1 effector PICK1 is needed for exocytosis and recruitment of Exo70 during InlB-dependent uptake. Interestingly, PICK1 does not accumulate in endomembranes with VAMP3, suggesting that PICK1 does not translocate to the plasma membrane through RE-mediated exocytosis. PICK1 contains a BAR domain capable of binding lipids and a PDZ domain that interacts with activated Arf1 and several other proteins, including neurotransmitter receptors, transporters, and the serine/threonine kinase protein kinase C-α (PKC-α) (56–58). Like PICK1, PKC-α controls exocytosis during InlB-mediated entry (7). In addition, both PKC-α and PICK1 are needed for recruitment of Exo70, but not FlnA, during entry. It therefore seems plausible that PICK1 and PKC-α act together to promote exocytosis through mobilization of Exo70. The mechanism by which PICK1 and PKC-α control Exo70 localization is presently unknown. The observations that PICK1 and PKC-α do not

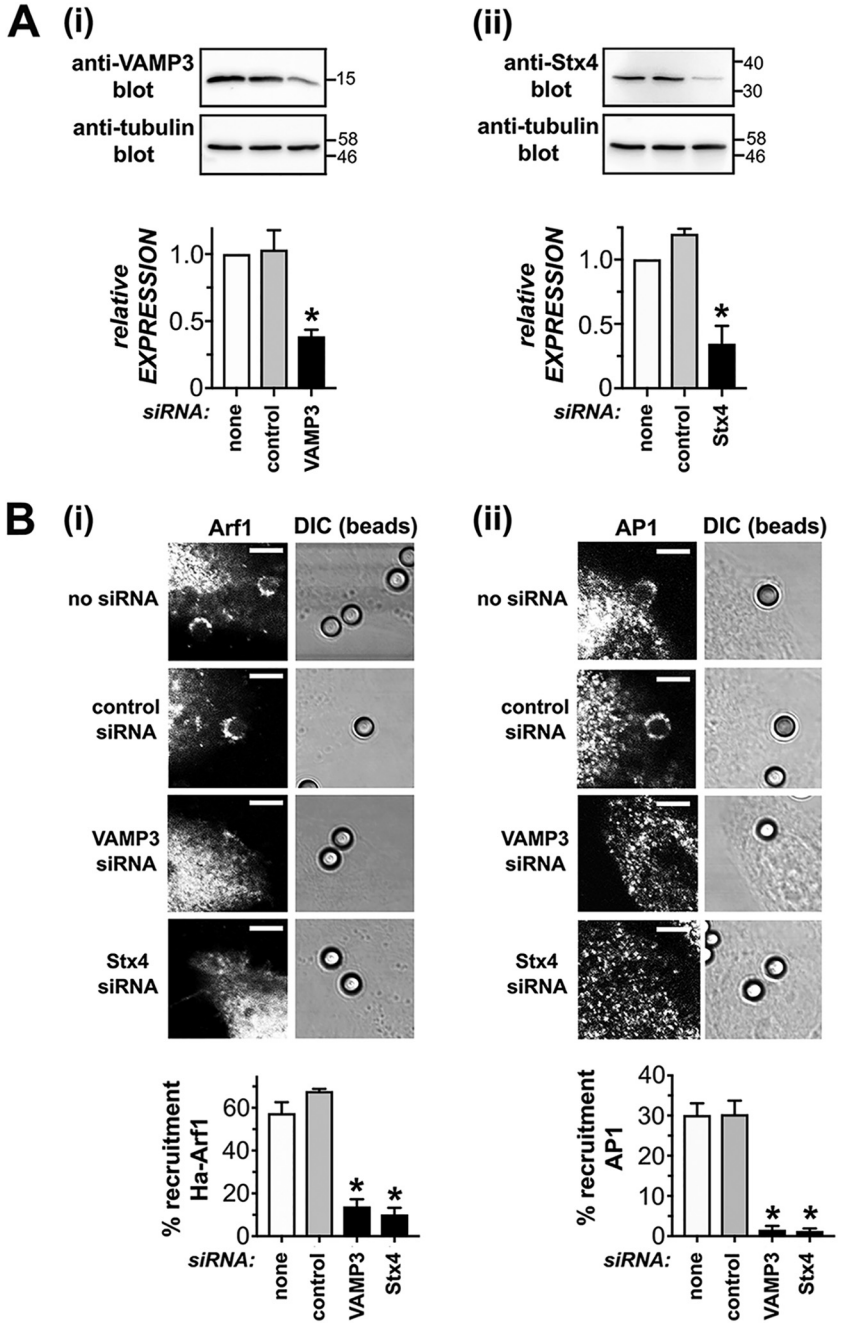

FIG 11 Translocation of Arf1 and AP1 to the plasma membrane requires SNARE proteins. HeLa cells were transiently mock transfected in the absence of siRNA, transfected with a control nontargeting siRNA, or transfected with siRNAs against the v-SNARE protein VAMP3 or the t-SNARE Stx4. Cells were then transfected with plasmids expressing HA-Arf1 or HA-AP1, followed by incubation with InlB-coated beads for 5 min. Samples were fixed and labeled for HA-tagged Arf1 or AP1. (A) Confirmation that siRNAs deplete VAMP3 and Stx4. Images of representative Western blots for VAMP3 (i) or Stx4 (ii) are shown in the top panels. The bar graphs below the Western blot images are quantified Western blotting data expressed as mean relative expression values ± SEM from three experiments. *, $P < 0.05$. (B) Effect of siRNAs against VAMP3 or Stx4 on recruitment of HA-tagged Arf1 or endogenous AP1. (i) Representative confocal microscopy images are presented. DIC indicates differential interference contrast images. Scale bars represent 5 μm. (ii) Quantification of effects of VAMP3 or Stx4 RNAi on recruitment of HA-Arf1 or AP1. Data are means ± SEM from three experiments. In each experiment, approximately 50 to 100 cell-associated beads were scored for each condition. *, $P < 0.05$ compared to the no siRNA or control siRNA conditions for InlB-coated beads.

affect mobilization of FlnA during InlB-dependent entry suggests that FlnA and PICK1/PKC-α cooperate to mediate recruitment of the exocyst complex.

In addition to controlling exocytosis, Arf1, AP1, and PICK1 promote the accumulation of actin filaments during InlB-dependent entry. Interestingly, PICK1 is known to regulate actin filament assembly through interactions with the Arp2/3 complex (59) and/or the GTPases Rac1 and Cdc42 (57). Future work should determine the extent to which these interactions control the actin cytoskeleton during InlB-mediated uptake. How AP1 might regulate actin polymerization is presently unclear.

In this study, we found that the Arf1 effector PIP5K1A contributed to InlB-mediated entry and actin cytoskeletal changes. These results are in general agreement with the known role of the PIP5K1A product phosphatidylinositol 4,5-bisphosphate (PIP2) in actin polymerization (60). In contrast, PIP5K1A was dispensable for exocytosis and mobilization of FlnA or Exo70 during entry. The lack of effect of PIP5K1A on recruitment of Exo70 is somewhat surprising given that PIP2 is known to bind this exocyst component (15). However, PIP5K1A is only one of three mammalian type I phosphatidylinositol 4-phosphate 5-kinases (PI4P5Ks) that are capable of synthesizing PIP2 (25). Apart from PI4P5Ks, PIP2 can also by produced by PI5P4Ks. It therefore seems plausible that RNAi-mediated depletion of PIP5K1A does not sufficiently reduce PIP2 levels to the extent that would perturb recruitment of Exo70. In this work, we were unable to assess localization of PIP5K1A. Therefore, it is presently unclear if this lipid kinase controls InlB-mediated entry by acting on an Arf1-dependent or -independent pathway. In this regard, it is worth noting that PIP5K1A can be activated not only by Arf1 but also by Rac1 and Cdc42 (60), small GTPases that promote InlB-dependent entry (8).

Our previous findings indicate that actin polymerization and exocytosis are separable host physiological responses during InlB-dependent entry of *Listeria* (6). Specifically, inhibition of actin polymerization fails to reduce exocytosis around InB-coated beads, and impairment of exocytosis fails to decrease F-actin accumulation around beads. Although exocytosis and actin polymerization are separable, each of these host processes is essential for InlB-mediated entry (4–6, 8). It would therefore seem advantageous for these two host processes to be coordinated temporally and spatially in order to achieve optimal InlB-mediated uptake. The results of this study demonstrate that Arf1 is a key regulator capable of coordinating exocytosis and F-actin remodeling to promote efficient infection by *Listeria*.

Finally, we note that Arf family GTPases control the entry of several bacterial pathogens apart from *Listeria*. Internalization of the Gram-negative bacteria *Yersinia pseudotuberculosis*, *Chlamydia caviae*, *Shigella flexneri*, and *Salmonella enterica* serovar Typhimurium all involve exploitation of host Arf6 (41, 48, 61–63). Interestingly, entry of *Salmonella* also requires Arf1, which is activated in an Arf6-dependent fashion during infection (41, 48). To date, work with *Yersinia*, *Chlamydia*, *Shigella*, and *Salmonella* have focused on the roles of Arf proteins in mediating actin cytoskeletal rearrangements during bacterial uptake. An interesting question is whether future work will reveal important functions for Arf proteins in controlling exocytosis during infection by these pathogens.

MATERIALS AND METHODS

Bacterial strains, mammalian cell lines, and media. The *Listeria monocytogenes* strain BUG 947 was grown in brain heart infusion (BHI; Difco) broth and prepared for infection as described previously (46). This strain was derived from the wild-type strain EGD, contains an in-frame deletion in the *inlA* gene, and is internalized into mammalian cells in a manner dependent on the *Listeria* protein InlB and its host receptor, Met (3, 29, 64).

The human epithelial cell line HeLa (ATCC CCL-2) was grown in Dulbecco's modified Eagle medium (DMEM) with 4.5 g of glucose per liter and 2 mM glutamine (catalog no. 11995-065; Life Technologies), supplemented with 5 or 10% fetal bovine serum (FBS). Cell growth, bacterial infections, incubations with latex beads, and stimulation with InlB protein were performed at 37°C under 5% CO_2.

Antibodies, inhibitors, and purified proteins. Rabbit antibodies used were anti-glutathione *S*-transferase (anti-GST, G7781; Sigma-Aldrich) and anti-InlB (3). Mouse monoclonal antibodies used were anti-AP1 (gamma 1 adaptin; sc-398867; Santa Cruz Biotechnology), anti-Arf1 (MAB3779; Chemicon),

anti-Exo70 (ED2001; Kerafast), anti-Filamin A (Millipore; CBL228), anti-GFP (11814460001; Sigma-Aldrich), anti-hemagglutinin (HA) (MMS-101P; Covance), anti-myc (9E10) (626802; BioLegend), and anti-tubulin (T5168; Sigma-Aldrich). Horseradish peroxidase-conjugated secondary antibodies were purchased from Jackson Immunolabs. Secondary antibodies or phalloidin coupled to Alexa Fluor 488, Alexa Fluor 555, or Alexa Fluor 647 were obtained from Life Technologies. 6×His-tagged InlB or GST proteins were expressed in *Escherichia coli* and purified as previously described (46, 65).

siRNAs. The sequences of short interfering RNAs (siRNAs) used were 5′-GAAGUUAUGUUCGUGAUG Att-3′ (AP1-1), 5′-CCACAAAUGGCCCUACUGAtt-3′ (AP1-2), 5′-CUGUAUCAAGAAUGAUCUUtt-3′ (AP1-3), 5′-GCCUGAUCUUCGUGGUGGAtt-3′ (Arf1-1), 5′-GGCUUUAGAGCUGUGUUGAtt-3′ (Arf1-2), 5′-CCUCUUGC CCUCUGCUUUAtt-3′ (Arf1-3), 5′-GAGACAGUGGAGUAUAAGAtt-3′ (Arf3-1), 5′-GAAAGACCACCAUCCUAU Att-3′ (Arf3-2), 5′-CAAUGAUCGGGAGCGAGUAtt-3′ (Arf3-3), 5′-CAGAAUACCCAGGGUCUUAtt-3′ (Arf4-1), 5′-GAUGUUGGUGGUCAAGAUAtt-3′ (Arf4-2), 5′-GACUUGACUGGCUGUCAAAtt-3′ (Arf4-3), 5′-CUCAUCUU UGUGGUGGACAtt-3′, (Arf5-1), 5′-GGAUGCAGUGCUGCUGGUAtt-3′ (Arf5-2), 5′-GCCUCAUCUUUGUGGUG GAtt-3′ (Arf5-3), 5′-CAUUAUGACCGGGCUCAUAtt-3′ (clathrin heavy chain), 5′-CCAGAGACAUGUAUGAU AAuu-3′ (Met), 5′-GCGAUGAGAUCACCGGUGUtt-3′ (PICK1-1), 5′-GACACUCGCCUCACCAUCAtt-3′ (PICK1-2), 5′-GUGUCAAUGGCAGGUCAAUtt-3′ (PICK1-3), 5′-CUCAGAAGACCUGGAACAAtt-3′ (PIP5K1A-1), 5′-AC ACAGUACUCAGUUGAUAuu-3′ (PIP5K1A-2), 5′-CCAACAUAAAGAGGCGGAAtt-3′ (PIP5K1A-3), 5′-GCAAUU CAAUGCAGUCCGAtt-3′ (Stx4), and 5′-GGGAUUACUGUUCUGGUUAtt-3′ (VAMP3). (Lowercase letters indicate nucleotide overhangs that are not complementary to targeted gene sequences.) These siRNAs were obtained from Sigma-Aldrich. The negative, nontargeting control siRNA molecule 1 (catalog no. D-001210-01) was purchased from Dharmacon. This siRNA has two or more mismatches with all sequences in the human genome, indicating that it should not target host mRNAs.

Mammalian expression plasmids. Mammalian expression vectors used were pcDNA-HA-Arf1 (48), pcDNA-HA-Arf1.Q71L (41), pcDNA-HA-Arf1.T31N (41), pcDNA-HA-gamma adaptin 1 (AP1) (Addgene number 10712; gift of William Sellers), pEBB-HA-luciferase (47), pEGFP-C3-Exo70 (Addgene number 53761; gift of Channing Der), pRK5-myc-PICK1 (Addgene number 72573; gift of Victor Anggono), and VAMP3-GFP (52).

Transfection. HeLa cells grown in 24-well plates or on 22- by 22-mm coverslips were transfected with siRNAs or plasmid DNA using Lipofectamine 2000 (Life Technologies) as previously described (29, 65, 66).

qPCR analysis. Samples were prepared for quantitative PCR (qPCR) as described previously (35). qPCR was performed in triplicate on each cDNA sample using an ABI7500 or ABI7900 instrument. TaqMan probes (Thermo Fisher Scientific) used for detection of gene expression were Hs00153910_m1 (AP1), Hs00992773_g1 (Arf3), Hs01070798_g1 (Arf4), Hs01018622_m1 (Arf5), Hs00202661_m1 (PICK1), and Hs00801004_s1 (PIP5K1A). The glyceraldehyde-3-phosphate dehydrogenase (GAPDH) gene (probe Hs99999905_m1) was used as an endogenous control. Data were analyzed by the comparative threshold cycle (C_T) method, normalizing C_T values for target gene expression to those for GAPDH. Relative quantity (RQ) values were calculated by the formula $RQ = 2^{-\Delta\Delta CT}$. To obtain the relative expression values shown in Fig. S1 and S4 in the supplemental material, RQ values in a given experiment were normalized to values in cells mock transfected in the absence of siRNA (no siRNA condition). The data shown in Fig. S1 and S4 are means ± standard errors of the means (SEM) from 3 to 4 independent experiments, depending on the gene and siRNA condition.

Western blotting. HeLa cells were solubilized in radioimmunoprecipitation assay (RIPA) buffer (1% Triton X-100, 0.25% sodium deoxycholate, 0.05% SDS, 50 mM Tris-HCl [pH 7.5], 2 mM EDTA, 150 mM NaCl, 1 mM phenylmethylsulfonyl fluoride, and 10 mg/liter each of aprotinin and leupeptin). Protein concentrations of lysates were determined using a bicinchoninic acid (BCA) assay kit (Pierce), and equal protein amounts of each sample were migrated on 7.5% or 12% SDS-polyacrylamide gels. Transfer of proteins to polyvinylidene (PVDF) membranes, incubation with primary antibodies or secondary antibodies coupled to horseradish peroxidase, and detection using enhanced chemiluminescence (ECL) or ECL Plus reagents (GE Healthcare) were performed as described previously (3). Chemiluminescence was detected using an Odyssey imaging system (Li-Cor Biosciences). Bands in Western blot images were quantified using ImageJ software, as described elsewhere (67).

Surface biotinylation studies. Surface Met was detected using a previously described approach involving biotinylating surface proteins using the membrane-impermeable reagent EZ-Link Sulfo-NHS-SS-Biotin (Thermo Fisher Scientific), isolating biotinylated proteins from solubilized extracts by precipitation with streptavidin-agarose beads, and detection of Met in precipitates by Western blotting (6, 50, 51). Prior to biotinylation, HeLa cells grown in 6-well plates were either mock transfected in the absence of siRNA, transfected with a control nontargeting siRNA, or transfected with siRNAs against Arf1 or AP1. Biotinylation and isolation of biotinylated proteins with streptavidin agarose were performed about 48 h after siRNA transfection.

Coupling of proteins to latex beads. InlB or GST proteins were coupled to carboxylate-modified latex beads 3 μm in diameter (catalog no. 09850; Polysciences) using either passive binding or covalent linkage, as described previously (6, 29).

Stimulation with soluble InlB protein. HeLa cells were placed in DMEM without FBS for 1 h, followed by addition of 300 ng/ml (4.5 nM) soluble InlB for 5 min at 37°C in 5% CO_2. Cells were then washed in cold phosphate-buffered saline (PBS), and lysates were prepared for detection of Arf1-GTP.

Measurement of Arf1-GTP. Levels of Arf1-GTP in HeLa cells were measured using an established approach that detects coprecipitation of Arf1 with a GST fusion protein containing the VHS and Arf binding domain of the effector GGA3 (43–45). For experiments involving HeLa cells stimulated with soluble InlB or expressing HA-tagged Arf1 proteins, coprecipitation with GST-GGA3 or GST was per-

formed exactly as previously described (43). In the case of experiments involving loading lysates with GTPγS or GDP, approximately 1 mg of lysate was incubated in the absence of nucleotide or with 1 mM GTPγS or 5 mM GDP at room temperature for 30 min prior to precipitation with GST-GGA3 or GST. Precipitates were then migrated on 12% SDS-PAGE gels and Arf1 was detected by Western blotting.

Bacterial entry assays. Entry of *Listeria* was measured using gentamicin protection assays, as previously described (3, 35). HeLa cells were infected with *Listeria* approximately 48 h after transfection with siRNAs. Cells were infected for 1 h in the absence of gentamicin using a multiplicity of infection of 30:1 and then incubated in DMEM with 20 μg/ml gentamicin for an additional 2 h. Bacterial entry efficiencies were first expressed as the percentage of the inoculum that survived gentamicin treatment. To obtain relative entry values, absolute percent entry values in a given experiment were normalized to the value in cells subjected to mock transfection in the absence of siRNA.

Quantification of internalization of beads. Beads coated with InlB or GST were added to HeLa cells growing on 22- by 22-mm coverslips. A ratio of approximately 5 particles to human cells was used. Cells were centrifuged at 1,000 rpm for 2 min at room temperature and then incubated for 30 min at 37°C in 5% CO_2 to allow internalization of beads. Cells then were washed in PBS and fixed in PBS containing 3% paraformaldehyde (PFA). Samples were labeled with anti-InlB or anti-GST antibodies, using a previously described approach that distinguishes extracellular or intracellular particles (29). In the case of experiments involving HA-tagged Arf1 proteins, samples were also labeled with mouse anti-HA antibodies to allow identification of transfected cells. Secondary antibodies used for labeling were coupled to Alexa Fluor 488, Alexa Fluor 555, and Alexa Fluor 647. Labeled samples were mounted in Mowiol with 1,4-diazabicyclo[2.2.2]octane (DABCO) as an antifade agent. Samples were analyzed for intracellular and extracellular beads using an Olympus BX51 epifluorescence microscope equipped with a 20×, 0.75-numeric-aperture (NA) dry lens objective and an Olympus DP80 charge-coupled device camera, using Olympus cellSens software (version 1.13). Results shown in Fig. 1B are from three experiments. In each experiment, approximately 200 cell-associated beads coated with InlB or 50 beads associated with GST were analyzed for entry. The data shown in Fig. 1C and D and Fig. S3 are from 3 to 4 experiments. In each experiment, approximately 100 cell-associated beads were scored for each condition. Data were initially expressed as the percentage of total cell-associated beads that were internalized. These data were then converted to relative internalization values by normalizing to percent internalization data from controls lacking siRNA (Fig. 1C and Fig. S3) or expressing HA-luciferase (Fig. 1D).

Confocal microscopy analysis. For studies involving recruitment of HA-tagged Arf1 and/or YFP-NGAT to beads (Fig. 3), HeLa cells grown on 22- by 22-mm coverslips were transfected with plasmid DNA for about 24 h. Cells were then washed and placed in serum-free DMEM. Beads coated with InlB or GST were added to cells at a ratio of about 5 particles per human cell. The cells were centrifuged at 1,000 rpm for 2 min to enhance contact between beads and HeLa cells and then incubated for 5 min at 37°C in 5% CO_2. Cells were washed in PBS, fixed in PBS with 3% PFA, and permeabilized in PBS with 0.4% Triton X-100. HA-Arf1 was labeled using mouse antibodies against the HA epitope followed by anti-mouse Alexa Fluor 555 secondary antibodies.

Experiments involving recruitment of HA-Arf1, HA-AP1, myc-PICK1, or EGFP-Exo70, shown in Fig. 5, 10, and 11, were performed similarly to those described above, except that HeLa cells were transfected with siRNAs about 24 h prior to transfection with plasmid DNA. For samples used for Fig. 5 and 10, extracellular beads were labeled with rabbit antibodies against InlB or GST and secondary antibodies coupled to Alexa Fluor 647 prior to permeabilization of cells, as described previously (35). For samples used for Fig. 11, beads were not labeled. After permeabilization, cells expressing HA- or myc-tagged proteins were labeled with mouse antibodies against these epitopes and anti-mouse secondary antibodies coupled to Alexa Fluor 488. Samples expressing EGFP-Exo70 were not labeled with antibodies.

In the case of studies assessing accumulation of F-actin around beads, HeLa cells were incubated with beads about 48 h after transfection with siRNAs. Samples were labeled for extracellular beads and F-actin using phalloidin-Alexa Fluor 555, as previously described (34).

For experiments measuring exocytosis around beads, HeLa cells were transfected with siRNAs for ~24 h, followed by transfection with a plasmid expressing VAMP3-GFP for another ~24 h. After incubation with beads for 5 min, cells were washed in PBS and incubated with mouse anti-GFP antibodies for 1 h at 4°C. Cells were then fixed in PBS with 3% PFA and incubated with anti-mouse antibodies coupled to Alexa Fluor 647 for 1 h. This method resulted in labeling of exofacial VAMP3-GFP (6, 7, 52). Extracellular beads were labeled by incubation with anti-InlB or anti-GST antibodies, followed by secondary antibodies conjugated to Alexa Fluor 555.

For labeling of endogenous AP1, FlnA, or Exo70, cells were fixed by incubation in methanol for 5 min at −20°C. Samples were then incubated overnight at 4°C with mouse anti-AP1, anti-FlnA, or anti-Exo70 antibodies in PBS with 1.0% bovine serum albumin and 0.1% Tween 20. Cells were then incubated with anti-mouse antibodies coupled to Alexa Fluor 555.

All samples for confocal microscopy analysis were mounted in Mowiol supplemented with DABCO. Imaging was performed with a Zeiss LSM710 or an Olympus FV1200 laser scanning confocal microscope, using a 60 ×, 1.35-NA oil immersion objective, laser lines of 488 nm, 543 nm, and 633 nm, and photomultiplier tubes for detection. Images from serial sections spaced 1.0 μm apart were used to ensure that all cell-associated beads were detected. ImageJ (version 1.51e) software was used to visualize and quantify confocal microscopy images. In the case of Arf1 or Arf1 effectors, which are present predominantly in endomembranes (16), recruitment to beads was scored as the presence of a ring-like structure around particles at the plasma membrane (Fig. 3 and 5). For experiments quantifying actin polymerization, exocytosis, FlnA accumulation, or EGFP-Exo70 local-

ization around beads (Fig. 6 to 9), we determined fold enrichment (FE) values for each cell-associated bead. FE is defined as the mean pixel intensity in a ring-like structure around the bead normalized to the mean pixel intensity throughout the human cell (6, 7, 26, 34, 35). The thresholding function of Image J was used to measure mean pixel intensities in ring-like structures of F-actin, exofacial VAMP3-GFP, or EGFP-Exo70 around beads. This function was also used to measure mean pixel intensity throughout the cell. In each experiment, approximately 40 to 80 extracellular, cell-associated beads were analyzed for each condition. The data shown in Fig. 6B, 7B, 8B, and 9B are pooled FE values from three independent experiments.

Statistical analysis. Statistical analysis was performed using Prism (version 7.0; GraphPad Software). In comparisons of data from three or more conditions, analysis of variance (ANOVA) was used. The Tukey-Kramer test was used as a posttest. For comparisons of two data sets, Student's *t* test was used. A *P* value of 0.05 or lower was considered significant.

SUPPLEMENTAL MATERIAL

Supplemental material is available online only.

SUPPLEMENTAL FILE 1, PDF file, 2.7 MB.

ACKNOWLEDGMENTS

We thank Vassilis Koronakis (University of Cambridge) for mammalian expression plasmids. James Casanova (University of Virginia) is gratefully acknowledged for advice on the Arf1 activation assay.

This work was supported by grants from the Marsden Fund of the Royal Society of New Zealand (13-UOO-085), the Health Research Council of New Zealand (17/082), and the University of Otago Research Committee, awarded to K.I.

REFERENCES

1. Posfay-Barbe KM, Wald ER. 2009. Listeriosis. Semin Fetal Neonatal Med 14:228–233. https://doi.org/10.1016/j.siny.2009.01.006.
2. Disson O, Lecuit M. 2013. *In vitro* and *in vivo* models to study human listeriosis: mind the gap. Microbes Infect 15:971–980. https://doi.org/10.1016/j.micinf.2013.09.012.
3. Shen Y, Naujokas M, Park M, Ireton K. 2000. InlB-dependent internalization of *Listeria* is mediated by the Met receptor tyrosine kinase. Cell 103:501–510. https://doi.org/10.1016/s0092-8674(00)00141-0.
4. Pizarro-Cerda J, Kuhbacher A, Cossart P. 2012. Entry of *Listeria monocytogenes* in mammalian epithelial cells: an updated view. Cold Spring Harb Perspect Med 2:a010009. https://doi.org/10.1101/cshperspect.a010009.
5. Kühbacher A, Emmenlauer M, Rämo P, Kafai N, Dehio C, Cossart P, Pizarro-Cerdá J. 2015. Genome-wide siRNA screen identifies complementary signaling pathways involved in *Listeria* infection and reveals different actin nucleation mechanisms during *Listeria* cell invasion and actin comet tail formation. mBio 6:e00598-15. https://doi.org/10.1128/mBio.00598-15.
6. Van Ngo H, Bhalla M, Chen D-Y, Ireton K. 2017. A role for host cell exocytosis in InlB-mediated internalisation of *Listeria monocytogenes*. Cell Microbiol 19:e12768. https://doi.org/10.1111/cmi.12768.
7. Bhalla M, Van Ngo H, Gyanwali GC, Ireton K. 2018. The host scaffolding protein Filamin A and the exocyst complex control exocytosis during InlB-mediated entry of *Listeria monocytogenes*. Infect Immun 87:e00689-18. https://doi.org/10.1128/IAI.00689-18.
8. Ireton K, Rigano LA, Dowd GC. 2014. Role of host GTPases in infection by *Listeria monocytogenes*. Cell Microbiol 16:1311–1320. https://doi.org/10.1111/cmi.12324.
9. Hong WJ, Lev S. 2014. Tethering the assembly of SNARE complexes. Trends Cell Biol 24:35–43. https://doi.org/10.1016/j.tcb.2013.09.006.
10. Veiga E, Cossart P. 2005. *Listeria* hijacks the clathrin-dependent endocytic machinery to invade mammalian cells. Nat Cell Biol 7:894–900. https://doi.org/10.1038/ncb1292.
11. Daumke O, Roux A, Haucke V. 2014. BAR domain scaffolds in dynamin-mediated membrane fission. Cell 156:882–892. https://doi.org/10.1016/j.cell.2014.02.017.
12. Bierne H, Gouin E, Roux P, Caroni P, Yin HL, Cossart P. 2001. A role for cofilin and LIM kinase in *Listeria*-induced phagocytosis. J Cell Biol 155:101–112. https://doi.org/10.1083/jcb.200104037.
13. Bierne H, Miki H, Innocenti M, Scita G, Gertler FB, Takenawa T, Cossart P. 2005. WASP-related proteins, Abi and Ena/VASP are required for *Listeria* invasion induced by the Met receptor. J Cell Sci 118:1537–1547. https://doi.org/10.1242/jcs.02285.
14. Bosse T, Ehinger J, Czuchra A, Benesch S, Steffen A, Wu X, Schloen K, Niemann HH, Scita G, Stradal TEB, Brakebusch C, Rottner K. 2007. Cdc42 and phosphoinositide 3-kinase drive Rac-mediated actin polymerization downstream of c-Met in distinct and common pathways. Mol Cell Biol 27:6615–6628. https://doi.org/10.1128/MCB.00367-07.
15. Wu B, Guo W. 2015. The exocyst at a glance. J Cell Sci 128:2957–2964. https://doi.org/10.1242/jcs.156398.
16. Donaldson JG, Jackson CL. 2011. ARF family G proteins and their regulators: roles in membrane transport, development, and disease. Nat Rev Mol Cell Biol 12:362–375. https://doi.org/10.1038/nrm3117.
17. Jackson CL, Bouvet S. 2014. Arfs at a glance. J Cell Sci 127:4103–4109. https://doi.org/10.1242/jcs.144899.
18. Singh V, Davidson AC, Hume PJ, Humphreys D, Koronakis V. 2017. Arf GTPase interplay with Rho GTPases in regulation of the actin cytoskeleton. Small GTPases 10:411–418. https://doi.org/10.1080/21541248.2017.1329691.
19. Kondo Y, Hanai A, Nakai W, Katoh Y, Nakayama K, Shin HW. 2012. Arf1 and Arf3 are required for the integrity of recycling endosomes and the recycling pathway. Cell Struct Funct 37:141–154. https://doi.org/10.1247/csf.12015.
20. Sathe M, Muthukrishnan G, Rae J, Disanza A, Thattai M, Scita G, Parton RG, Mayor R. 2018. Small GTPases and BAR domain proteins regulate branched actin polymerisation for clathrin and dynamin-independent endocytosis. Nat Commun 9:1835. https://doi.org/10.1038/s41467-018-03955-w.
21. Rocca DL, Martin S, Jenkins EL, Hanley JG. 2008. Inhibition of Arp2/3-dependent actin polymerisation by PICK1 regulates neuronal morphology and AMPA receptor endocytosis. Nat Cell Biol 10:259–271. https://doi.org/10.1038/ncb1688.
22. Moravec R, Conger KK, D'Souza R, Allison AB, Casanova JE. 2012. BRAG2/GEP100/IQSec1 interacts with clathrin and regulates $\alpha 5\beta 1$ integrin endocytosis through activation of ADP ribosylation factor 5 (Arf5). J Biol Chem 287:31138–31147. https://doi.org/10.1074/jbc.M112.383117.
23. Nakatsu F, Hase K, Ohno H. 2014. The role of clathrin adaptor AP-1: polarized sorting and beyond. Membranes 4:747–763. https://doi.org/10.3390/membranes4040747.
24. Paczkowski JE, Richardson BC, Fromme JC. 2015. Cargo adaptors: structures illuminate mechanisms regulating vesicle biogenesis. Trends Cell Biol 25:408–416. https://doi.org/10.1016/j.tcb.2015.02.005.
25. Perez-Mansilla B, Ha VL, Justin N, Wilkins AJ, Carpenter CL, Thomas G. 2006. Differential regulation of phosphatidylinositol 4-phosphate 5-kinases and phospholipase D1 by ADP-ribosylation factors 1 and 6.

Biochim Biophys Acta 1761:1429–1442. https://doi.org/10.1016/j.bbalip.2006.09.006.
26. Gavicherla B, Ritchey L, Gianfelice A, Kolokoltsov AA, Davey RA, Ireton K. 2010. Critical role for the host GTPase-activating protein ARAP2 in InlB-mediated entry of *Listeria monocytogenes*. Infect Immun 78:4532–4541. https://doi.org/10.1128/IAI.00802-10.
27. Yoon HY, Miura K, Cuthbert EJ, Davis KK, Ahvazi B, Casanova JE, Randazzo PA. 2006. ARAP2 effects on the actin cytoskeleton are dependent on Arf6-specific GTPase-activating-protein activity and binding to RhoA-GTP. J Cell Sci 119:4650–4666. https://doi.org/10.1242/jcs.03237.
28. Ireton K, Payrastre B, Chap H, Ogawa W, Sakaue H, Kasuga M, Cossart P. 1996. A role for phosphoinositide 3-kinase in bacterial invasion. Science 274:780–782. https://doi.org/10.1126/science.274.5288.780.
29. Dokainish H, Gavicherla B, Shen Y, Ireton K. 2007. The carboxyl-terminal SH3 domain of the mammalian adaptor CrkII promotes internalization of *Listeria monocytogenes* through activation of host phosphoinositide 3-kinase. Cell Microbiol 9:2497–2516. https://doi.org/10.1111/j.1462-5822.2007.00976.x.
30. Mohr SE, Smith JA, Shamu CE, Neumuller RA, Perrimon N. 2014. RNAi screening comes of age: improved techniques and complementary approaches. Nat Rev Mol Cell Biol 15:591–600. https://doi.org/10.1038/nrm3860.
31. Braun L, Ohayon H, Cossart P. 1998. The InlB protein of Listeria monocytogenes is sufficient to promote entry into mammalian cells. Mol Microbiol 27:1077–1087. https://doi.org/10.1046/j.1365-2958.1998.00750.x.
32. Seveau S, Bierne H, Giroux S, Prevost MC, Cossart P. 2004. Role of lipid rafts in E-cadherin- and HGF-R/Met-mediated entry of *Listeria monocytogenes* into host cells. J Cell Biol 166:743–753. https://doi.org/10.1083/jcb.200406078.
33. Veiga E, Guttman JA, Bonazzi M, Boucrot E, Toledo-Arana A, Lin AE, Enninga J, Pizarro-Cerdá J, Finlay BB, Kirchhausen T, Cossart P. 2007. Invasive and adherent bacterial pathogens co-opt hos clathrin for infection. Cell Host Microbe 2:340–351. https://doi.org/10.1016/j.chom.2007.10.001.
34. Bhalla M, Law D, Dowd GC, Ireton K. 2017. Host serine/threonine kinases mTOR and protein kinase C-alpha promote InlB-mediated entry of *Listeria monocytogenes*. Infect Immun 85:e00087-17. https://doi.org/10.1128/IAI.00087-17.
35. Dowd GC, Bhalla M, Kean B, Thomas R, Ireton K. 2016. Role of host type IA phosphoinositide 3-kinase pathway components in invasin-mediated internalization of *Yersinia enterocolitica*. Infect Immun 84:1826–1841. https://doi.org/10.1128/IAI.00142-16.
36. Shin HW, Morinaga N, Noda M, Nakayama K. 2004. Arf1 and Arf4 regulate recycling endosomal morphology and retrograde transport from endosomes to the Golgi apparatus. Mol Biol Cell 15:5283–5294. https://doi.org/10.1091/mbc.e04-05-0388.
37. Beemiller P, Hoppe AD, Swanson JA. 2006. A phosphatidylinositol-3-kinase-dependent signal transition regulates Arf1 and Arf6 during Fcgamma receptor-mediated phagocytosis. PLoS Biol 4:e162. https://doi.org/10.1371/journal.pbio.0040162.
38. Braun V, Deschamps C, Raposo B, Benaroch P, Benmerah A, Chavrier P, Niedergang F. 2007. AP-1 and Arf1 control endosome dynamics at sites of FcR-mediated phagocytosis. Mol Biol Cell 18:4921–4931. https://doi.org/10.1091/mbc.e07-04-0392.
39. Kumari S, Mayor S. 2008. Arf1 is directly involved in dynamin-independent endocytosis. Nat Cell Biol 10:30–41. https://doi.org/10.1038/ncb1666.
40. Boulay PL, Schlienger S, Saravalli-Lewis S, Vitale N, Ferbeyre G, Claing A. 2011. Arf1 controls proliferation of breast cancer cells by regulating the retinoblastoma protein. Oncogene 30:3846–3861. https://doi.org/10.1038/onc.2011.100.
41. Davidson AC, Humphreys D, Brooks ABE, Hume PJ, Koronakis V. 2015. The Arf GTPase-activating protein family is exploited by *Salmonella enterica* serovar Typhimurium to invade nonphagocytic host cells. mBio 6:e02253-14. https://doi.org/10.1128/mBio.02253-14.
42. Casanova JE. 2007. Regulation of Arf activation: the Sec7 family of guanine nucleotide exchange factors. Traffic 8:1476–1485. https://doi.org/10.1111/j.1600-0854.2007.00634.x.
43. Santy LC, Casanova JE. 2001. Activation of Arf6 by ARNO stimulates epithelial cell migration through downstream activation of both Rac and phospholipase D. J Cell Biol 154:599–610. https://doi.org/10.1083/jcb.200104019.
44. Boulay PL, Cotton M, Melancon P, Claing A. 2008. ADP ribosylation factor 1 controls the activation of the phosphatidylinositol 3-kinase pathway to regulate epidermal growth factor-dependent growth and migration of breast cancer cells. J Biol Chem 283:36425–36434. https://doi.org/10.1074/jbc.M803603200.
45. Schlienger S, Campbell S, Claing A. 2014. Arf1 regulates the Rho/MLC pathway to control EGF-dependent breast cancer cell invasion. Mol Biol Cell 25:17–29. https://doi.org/10.1091/mbc.E13-06-0335.
46. Ireton K, Payrastre B, Cossart P. 1999. The *Listeria monocytogenes* protein InlB is an agonist of mammalian phosphoinositude-3-kinase. J Biol Chem 274:17025–17032. https://doi.org/10.1074/jbc.274.24.17025.
47. Sun H, Shen Y, Dokainish H, Holgado-Madruga M, Wong A, Ireton K. 2005. Host adaptor proteins Gab1 and CrkII promote InlB-dependent entry of *Listeria monocytogenes*. Cell Microbiol 7:443–457. https://doi.org/10.1111/j.1462-5822.2004.00475.x.
48. Humphreys D, Davidson AC, Hume PJ, Makin LE, Koronakis V. 2013. Arf6 coordinates actin assembly through the WAVE complex, a mechanism usurped by *Salmonella* to invade host cells. Proc Natl Acad Sci U S A 110:16880–16885. https://doi.org/10.1073/pnas.1311680110.
49. Takeya R, Takeshige K, Sumimoto H. 2000. Interaction of the PDZ domain of human PICK1 with class I ADP-ribosylation factors. Biochem Biophys Res Commun 267:149–1555. https://doi.org/10.1006/bbrc.1999.1932.
50. Li N, Xiang GS, Dokainish H, Ireton K, Elferink LA. 2005. The Listeria protein InlB mimics hepatocyte growth factor-induced receptor trafficking. Traffic 6:459–473. https://doi.org/10.1111/j.1600-0854.2005.00290.x.
51. Li N, Lorinczi M, Ireton K, Elferink LA. 2007. Specific Grb2-mediated interactions regulate clathrin-dependent endocytosis of the c-Met tyrosine kinase. J Biol Chem 282:16764–16775. https://doi.org/10.1074/jbc.M610835200.
52. Bajno L, Peng XR, Schreiber AD, Moore HP, Trimble WS, Grinstein S. 2000. Focal exocytosis of VAMP3-containing vesicles at sites of phagosome formation. J Cell Biol 149:697–705. https://doi.org/10.1083/jcb.149.3.697.
53. Futter CE, Gibson A, Allchin EH, Maxwell S, Ruddock LJ, Odorizzi G, Domingo D, Trowbridge IS, Hopkins CR. 1998. In polarized MDCK cells basolateral vesicles arise from clathrin-gamma-adaptin-coated domains on endosomal tubules. J Cell Biol 141:611–623. https://doi.org/10.1083/jcb.141.3.611.
54. Bonifacino JS. 2014. Adaptor proteins involved in polarized sorting. J Cell Biol 204:7–17. https://doi.org/10.1083/jcb.201310021.
55. Daro EA, van der Sluijs P, Galli T, Mellman I. 1996. Rab4 and cellubrevin define different early endosome populations on the pathway of transferrin receptor recycling. Proc Natl Acad Sci U S A 93:9559–9564. https://doi.org/10.1073/pnas.93.18.9559.
56. Erlendsson S, Rathje M, Heidarsson PO, Poulsen FM, Madsen KL, Teilum K, Gether U. 2014. Protein interacting with C-kinase 1 (PICK1) binding promiscuity relies on unconventional PSD-95/Discs-large/ZO-1 homology (PDZ) binding modes for nonclass II PDZ ligands. J Biol Chem 289:25327–25340. https://doi.org/10.1074/jbc.M114.548743.
57. Li YH, Zhang N, Wang YN, Shen Y, Wang Y. 2016. Multiple faces of protein interacting with kinase 1 (PICK1): structure, function, and diseases. Neurochem Int 98:115–121. https://doi.org/10.1016/j.neuint.2016.03.001.
58. Staudinger J, Lu J, Olson EN. 1997. Specific interaction of the PDZ domain protein PICK1 with the COOH terminus of protein kinase C-alpha. J Biol Chem 272:32019–32024. https://doi.org/10.1074/jbc.272.51.32019.
59. Rocca DL, Amici M, Antoniou A, Blanco Suarez E, Halemani N, Murk K, McGarvey J, Jaafari N, Mellor JR, Collingridge GL, Hanley JG. 2013. The small GTPase Arf1 modulates Arp2/3-mediated actin polymerization via PICK1 to regulate synaptic plasticity. Neuron 79:293–307. https://doi.org/10.1016/j.neuron.2013.05.003.
60. Zhang L, Mao YS, Janmey PA, Yin HL. 2012. Phosphtidylinositol 4,5 bis phosphate and the actin cytoskeleton. Subcell Biochem 59:177–215. https://doi.org/10.1007/978-94-007-3015-1_6.
61. Wong KW, Isberg RR. 2003. Arf6 and phosphoinositol-4-phosphate-5-kinase activities permit bypass of the Rac1 requirement for β1 integrin-mediated bacterial uptake. J Exp Med 198:603–614. https://doi.org/10.1084/jem.20021363.
62. Balana ME, Niedergang F, Subtil A, Alcover A, Chavrier P, Dautry-Varsat A. 2005. Arf6 GTPase controls bacterial invasion by actin remodeling. J Cell Sci 118:2201–2210. https://doi.org/10.1242/jcs.02351.
63. Garza-Mayers AC, Miller KA, Russo BC, Nagda DV, Goldberg MB. 2015. Shigella flexneri regulation of Arf6 activation during bacterial entry via an IpgD-mediated positive feedback loop. mBio 6:e02584-14. https://doi.org/10.1128/mBio.02584-14.

64. Dramsi S, Biswas I, Maguin E, Braun L, Mastroeni P, Cossart P. 1995. Entry of *Listeria monocytogenes* into hepatocytes requires expression of inlB, a surface protein of the internalin multigene family. Mol Microbiol 16:251–261. https://doi.org/10.1111/j.1365-2958.1995.tb02297.x.
65. Basar T, Shen Y, Ireton K. 2005. Redundant roles for Met docking site tyrosines and the Gab1 pleckstrin homology domain in InlB-mediated entry of *Listeria monocytogenes*. Infect Immun 73:2061–2074. https://doi.org/10.1128/IAI.73.4.2061-2074.2005.
66. Jiwani S, Wang Y, Dowd GC, Gianfelice A, Pichestapong P, Gavicherla B, Vanbennekom N, Ireton K. 2012. Identification of components of the type IA phosphoinositide 3-kinase pathway that promote internalization of *Listeria monocytogenes*. Infect Immun 80:1252–1266. https://doi.org/10.1128/IAI.06082-11.
67. Gianfelice A, Le PH, Rigano LA, Saila S, Dowd GC, McDivitt T, Bhattacharya N, Hong W, Stagg SM, Ireton K. 2015. Host endoplasmic reticulum COPII proteins control cell-to-cell spread of the bacterial pathogen *Listeria monocytogenes*. Cell Microbiol 17:876–892. https://doi.org/10.1111/cmi.12409.